0090-9556/06/3407-1229–1236$20.00
DRUG METABOLISM AND DISPOSITION

DMD 34:1229–1236, 2006

Vol. 34, No. 7
9290/3119191
Printed in U.S.A.

DRUG-DRUG INTERACTION BETWEEN PITAVASTATIN AND VARIOUS DRUGS VIA OATP1B1

Masaru Hirano, Kazuya Maeda, Yoshihisa Shitara, and Yuichi Sugiyama

Graduate School of Pharmaceutical Sciences, the University of Tokyo, Tokyo, Japan (M.H., K.M., Y.Su.); and Graduate School of Pharmaceutical Sciences, Chiba University, Chiba, Japan (Y.Sh.)

Received January 6, 2006; accepted March 29, 2006

ABSTRACT:

It has already been demonstrated that pitavastatin, a novel potent HMG-coenzyme A reductase inhibitor, is taken up into human hepatocytes mainly by organic anion transporting polypeptide (OATP) 1B1. Because OATP2B1 is also localized in the basolateral membrane of human liver, we took two approaches to further confirm the minor contribution of OATP2B1 to the hepatic uptake of pitavastatin. Western blot analysis revealed that the ratio of the band density of OATP2B1 in human hepatocytes to that in our expression system is at least 6-fold lower compared with OATP1B1 and OATP1B3. The uptake of pitavastatin in human hepatocytes could be inhibited by both estrone-3-sulfate (OATP1B1/OATP2B1 inhibitor) and estradiol-17β-D-glucuronide (OATP1B1/OATP1B3 inhibitor). These results further supported the idea that OATP1B1 is a predominant transporter for the hepatic uptake of pitavastatin. Then, to explore the possibility of OATP1B1-mediated drug-drug interaction, we checked the inhibitory effects of various drugs on the pitavastatin uptake in OATP1B1-expressing cells and evaluated whether the in vitro inhibition was clinically significant or not. As we previously reported, we used the methodology for estimating the maximum unbound concentration of inhibitors at the inlet to the liver ($I_{u,in,max}$). Judging from $I_{u,in,max}$ and inhibition constant (K_i) for OATP1B1, several drugs (especially cyclosporin A, rifampicin, rifamycin SV, clarithromycin, and indinavir) have potentials for interacting with OATP1B1-mediated uptake of pitavastatin. The in vitro experiments could support the clinically observed drug-drug interaction between pitavastatin and cyclosporin A. These results suggest that we should pay attention to the concomitant use of some drugs with pitavastatin.

The liver is one of the organs responsible for the elimination of xenobiotics including many kinds of drugs. In some cases, although the compounds were not supposed to easily penetrate the plasma membrane from the viewpoint of their physicochemical properties, they were efficiently taken up into liver and excreted into bile. Recently, it has been found that several kinds of transporters greatly help the efficient membrane transport of several compounds. It has been characterized that hepatic uptake of some of the compounds is mediated by organic anion-transporting polypeptide (OATP) family transporters, organic anion transporter 2, Na^+-taurocholate cotransporting polypeptide, and organic cation transporter 1 (Mizuno et al., 2003). Among these transporters, especially OATP1B1 and OATP1B3 are specifically expressed in liver and show broad substrate specificities (Hagenbuch and Meier, 2003). In contrast, OATP2B1 is also expressed in the basolateral membrane of human liver (Tamai et al., 2001). Previous reports indicated that the low pH facilitates the OATP2B1-mediated uptake of several organic anions, implying its involvement in the intestinal absorption of anions (Kobayashi et al., 2003). Although the uptake clearance at pH 7.4 was lower than that at pH 5.0, OATP2B1 could transport some organic anions such as estrone-3-sulfate, fexofenadine, benzylpenicillin, and dehydroepiandrosterone sulfate, even at pH 7.4 (Kobayashi et al., 2003; Nozawa et al., 2004). Therefore, it is possible that OATP2B1 is also involved in the hepatic uptake of anionic drugs.

Pitavastatin is a highly potent inhibitor of HMG-coenzyme A reductase, the rate-limiting enzyme in cholesterol biosynthesis (Aoki et al., 1997; Kajinami et al., 2003). Previously, Kimata et al. (1998) have revealed that [^{14}C]pitavastatin is selectively distributed to the liver in rats with the liver-to-plasma concentration ratio of more than 50, suggesting that active transport systems can be involved in the uptake of pitavastatin. We have already demonstrated that pitavastatin is taken up into human hepatocytes predominantly by OATP1B1, although it was a substrate of both OATP1B1 and OATP1B3 (Hirano et al., 2004). We also showed that the contribution of other transporters such as OATP2B1 to the pitavastatin uptake was theoretically small, but we have not experimentally shown the minor importance of OATP2B1. Therefore, we tried to confirm that OATP1B1 is a responsible transporter for the pitavastatin uptake by two kinds of approaches: the comparison of the expression level of each transporter in human hepatocytes and expression systems by Western blot analysis, and the inhibitory effects of transporter-selective inhibitors on the uptake of pitavastatin in human hepatocytes.

This work was supported by Health and Labour Sciences Research Grants from the Ministry of Health, Labour and Welfare for the Research on Advanced Medical Technology and a Grant-in Aid for Young Scientists (B) (15790087) from the Ministry of Education, Culture, Sports, Science and Technology.

Article, publication date, and citation information can be found at http://dmd.aspetjournals.org.

doi:10.1124/dmd.106.009290.

ABBREVIATIONS: HEK, human embryonic kidney; MDCK, Madin-Darby canine kidney; OATP, organic anion-transporting polypeptide; HMG-CoA, 3-hydroxy-3-methylglutaryl-coenzyme A; K_m, Michaelis constant; V_{max}, maximum transport velocity; K_i, inhibition constant; $E_2$17βG, estradiol 17β-D-glucuronide; E_1S, estrone-3-sulfate; DDI, drug-drug interaction.

The combination therapy of statins and various compounds is widely used in clinical practice. Coadministration of various drugs sometimes causes an increase in the plasma concentration of statins (Williams and Feely, 2002), which may occasionally lead to severe side effects such as myopathy and rhabdomyolysis (Evans and Rees, 2002). In the case of simvastatin, which is relatively lipophilic and metabolized by CYP3A4, itraconazole, cyclosporin A, and erythromycin were reported to increase plasma area under the plasma concentration-time curve of simvastatin by inhibition of CYP3A4-mediated metabolism (Kantola et al., 1998; Neuvonen et al., 1998; Ichimaru et al., 2001). In contrast, cyclosporin A also interacted with the nonmetabolized type of statins such as pravastatin, pitavastatin, and rosuvastatin in the clinical situation (Olbricht et al., 1997; Hasunuma et al., 2003; Simonson et al., 2004). Shitara et al. (2003) clarified that drug-drug interaction (DDI) between cyclosporin A and cerivastatin is caused by the inhibition of OATP1B1-mediated cerivastatin uptake by cyclosporin A. Because pitavastatin was reported to be taken up into hepatocytes mainly by OATP1B1 (Hirano et al., 2004), we should pay attention to the OATP1B1-mediated DDI of pitavastatin in coadministration with other drugs that can inhibit the function of OATP1B1. However, the inhibitors of OATP1B1 identified by in vitro analyses do not always cause DDI in the clinical situation when the clinical protein unbound concentration in plasma is much lower than the in vitro inhibition constant (K_i) for OATP1B1. Ito et al. (1998) proposed the calculation method for estimating the maximum unbound concentration of inhibitors at the inlet to the liver to avoid the false-negative prediction of clinical DDI.

In the present study, we confirmed the minor contribution of OATP2B1 to the hepatic uptake of pitavastatin by two approaches. Moreover, we tried to predict the possible DDI mediated by OATP1B1 between pitavastatin and various drugs by judging from the clinical maximum unbound concentration of each inhibitor in human plasma and the K_i value for OATP1B1 obtained from the in vitro study.

Materials and Methods

Materials. Pitavastatin, monocalcium bis[(3*R*,5*S*,6*E*)-7-[2-cyclopropyl-4-(4-fluorophenyl)-3-quinolyl]3,5-dihydroxy-6-hepteonate], was synthesized by Nissan Chemical Industries (Chiba, Japan). [^{3}H]Pitavastatin (16.0 Ci/mmol) was synthesized by GE Healthcare (Little Chalfont, Buckinghamshire, UK). [^{3}H]Estradiol 17β-D-glucuronide ($E_2$17βG) and [^{3}H]estrone-3-sulfate (E_1S) (45 Ci/mmol and 46 Ci/mmol, respectively) were purchased from New England Nuclear (Boston, MA). Unlabeled $E_2$17βG, E_1S, and gemfibrozil were purchased from Sigma-Aldrich (St. Louis, MO). A metabolite of gemfibrozil, M3 (purity 99.6%), was chemically synthesized at KNC Laboratories, Co. Ltd. (Kobe, Japan) as shown in detail previously (Shitara et al., 2004). All other chemicals were of analytical grade and commercially available.

Uptake Study Using Transporter Expression Systems. OATP1B1-, OATP1B3-, and OATP2B1-expressing HEK293 cells and vector-transfected control cells used in this study were constructed previously (Hirano et al., 2004; Shimizu et al., 2005). Transporter-expressing or vector-transfected HEK293 cells were grown in Dulbecco's modified Eagle's medium low glucose (Invitrogen, Carlsbad, CA) supplemented with 10% fetal bovine serum (Sigma-Aldrich), 100 U/ml penicillin, 100 μg/ml streptomycin, and 0.25 μg/ml amphotericin B at 37°C with 5% CO_2 and 95% humidity. Cells were then seeded in 12-well plates coated with poly-L-lysine/poly-L-ornithine at a density of 1.5×10^5 cells per well. After 2 days, the cell culture medium was replaced with culture medium supplemented with 5 mM sodium butyrate 24 h before transport assay to induce the expression of exogenous transporters. The transport study was carried out as described previously (Sugiyama et al., 2001). Uptake was initiated by adding Krebs-Henseleit buffer containing radiolabeled and unlabeled substrates after cells had been washed twice and preincubated with Krebs-Henseleit buffer at 37°C for 15 min. The Krebs-Henseleit buffer consisted of 118 mM NaCl, 23.8 mM $NaHCO_3$, 4.8 mM KCl, 1.0 mM KH_2PO_4, 1.2 mM $MgSO_4$, 12.5 mM HEPES, 5.0 mM glucose, and 1.5 mM $CaCl_2$ adjusted to pH 7.4. The uptake was terminated at a designated time by adding ice-cold Krebs-Henseleit buffer after removal of the incubation buffer. Then, cells were washed twice with 1 ml of ice-cold Krebs-Henseleit buffer, solubilized in 500 μl of 0.2 N NaOH, and kept overnight at 4°C. Aliquots (500 μl) were transferred to scintillation vials after adding 250 μl of 0.4 N HCl. The radioactivity associated with the cells and incubation buffer was measured in a liquid scintillation counter (LS6000SE; Beckman Coulter, Inc., Fullerton, CA) after adding 2 ml of scintillation fluid (Clear-sol I; Nacalai Tesque, Kyoto, Japan) to the scintillation vials. The remaining 50 μl of cell lysate was used to determine the protein concentration by the method of Lowry et al. (1951) with bovine serum albumin as a standard.

Uptake Study Using Human Cryopreserved Hepatocytes. This experiment was performed as described previously (Shitara et al., 2003). Cryopreserved human hepatocytes were purchased from In Vitro Technologies (Baltimore, MD). In this experiment, we selected three batches of human hepatocytes (lots OCF, 094, and ETR), which ranked in the top three of the uptake amount of $E_2$17βG, and E_1S among eight independent batches of hepatocytes. Immediately before the study, the hepatocytes (1-ml suspension) were thawed at 37°C, quickly suspended in 10 ml of ice-cold Krebs-Henseleit buffer, and centrifuged (50*g*) for 2 min at 4°C, followed by removal of the supernatant. This procedure was repeated once more to remove cryopreservation buffer, and then the cells were resuspended in the same buffer to give a cell density of 1.0×10^6 viable cells/ml for the uptake study. The number of viable cells was determined by trypan blue staining. Before the uptake studies, the cell suspensions were prewarmed in an incubator at 37°C for 3 min. The uptake studies were initiated by adding an equal volume of buffer containing radiolabeled and unlabeled pitavastatin to the cell suspension. After incubation at 37°C for 0.5 and 2 min, the reaction was terminated by separating the cells from the buffer. For this purpose, an aliquot of 80 μl of incubation mixture was collected and placed in a centrifuge tube (450 μl) containing 50 μl of 2 N NaOH under a layer of 100 μl of oil (density, 1.015; a mixture of silicone oil and mineral oil; Sigma-Aldrich), and subsequently the sample tube was centrifuged for 10 s using a tabletop centrifuge (10,000*g*; Beckman Microfuge E; Beckman Coulter, Inc.). During this process, hepatocytes passed through the oil layer into the alkaline solution. After an overnight incubation in alkali to dissolve the hepatocytes, the centrifuge tube was cut and each compartment was transferred to a scintillation vial. The compartment containing the dissolved cells was neutralized with 50 μl of 2 N HCl, mixed with scintillation cocktail, and the radioactivity was measured in a liquid scintillation counter.

Antiserum and Western Blot Analysis. As shown in previous reports, anti-OATP2B1 sera were raised in rabbits against a synthetic peptide consisting of the 15 carboxyl-terminal amino acids of OATP2B1 (LLVSGPGKKPEDSRV) coupled to keyhole limpet hemocyanine at its N-terminal via an additional cysteine (Kullak-Ublick et al., 2001). Crude membrane fractions were prepared from human hepatocytes and transporter-expressing HEK293 cells as described previously (Sasaki et al., 2002). The human liver block (lot 020188) was obtained from Human and Animal Bridging Research Organization (Chiba, Japan), and crude membrane fractions were prepared as described previously (Hirano et al., 2004). The samples were diluted with 3× Red loading buffer (BioLabs, Hertfordshire, UK) and loaded onto a 7% SDS-polyacrylamide gel with a 4.4% stacking gel. Proteins were electroblotted onto a polyvinylidene difluoride membrane (Pall, East Hills, NY) using a blotter (Trans-blot; Bio-Rad, Richmond, CA) at 15 V for 1 h. The membrane was blocked with Tris-buffered saline containing 0.05% Tween 20 (TBS-T) and 5% skimmed milk for 1 h at room temperature. After washing with TBS-T, the membrane was incubated with anti-OATP2B1 serum (dilution 1:1000). The membrane was incubated with a horseradish peroxidase-labeled anti-rabbit IgG antibody (GE Healthcare) diluted 1:5000 in TBS-T for 1 h at room temperature, followed by washing with TBS-T. The band was detected and its intensity was quantified using an image analyzer (LAS-1000 plus; Fuji Film, Tokyo, Japan).

Transcellular Transport Study. OATP1B1-, OATP1B1/BCRP-, OATP1B1/MDR1-, and OATP1B1/MRP2-expressing MDCKII cells and vector-transfected control cells used in this study were constructed previously (Matsushima et al., 2005). Transporter-expressing or vector-transfected MDCKII cells were grown in Dulbecco's modified Eagle's medium low glucose supplemented with 10% fetal bovine serum, 100 U/ml penicillin, 100

μg/ml streptomycin, and 0.25 μg/ml amphotericin B at 37°C with 5% CO_2 and 95% humidity. MDCKII cells were seeded on Transwell membrane inserts (6.5-mm diameter, 0.4-μm pore size; Corning Costar, Bodenheim, Germany) at a density of 1.4×10^5 cells per well. After 3 days, medium was replaced with 5 mM sodium butyrate for 24 h before the transport study (Sasaki et al., 2002). The experiments were initiated by replacing the medium on the basal side of the cell layer with Krebs-Henseleiti buffer containing radiolabeled and unlabeled pitavastatin (0.3 μM). The cells were incubated at 37°C, and aliquots of medium were taken from each compartment at designated time points. Radioactivity in 100 μl of medium was measured in a liquid scintillation counter after the addition of scintillation cocktail. At the end of the experiments, the cells were washed three times with 1.5 ml of ice-cold Krebs-Henseleit buffer and solubilized in 500 μl of 0.2 N NaOH. After addition of 100 μl of 1 N HCl, 500-μl aliquots were transferred to scintillation vials. Aliquots (50-μl) of cell lysate were used to determine protein concentrations as described above. To evaluate the efflux transport clearance via recombinant BCRP, MDR1, and MRP2 in the double transfectants, the apparent efflux clearance across the apical membrane (PS_{apical}) was calculated by dividing the steady-state velocity for the transcellular transport ($V_{transcellular}$) of pitavastatin, determined over 3 h, by the intracellular concentration (C_{cell}) of pitavastatin, determined at the end of the experiments (3 h) in the absence or presence of the inhibitors.

$$PS_{apical} = V_{transcellular}/C_{cell} \quad (1)$$

Kinetic Analyses. Ligand uptake in transporter cDNA-transfected cells was expressed as the uptake volume (μl/mg protein), given as the amount of radioactivity associated with the cells (dpm/mg protein) divided by its concentration in the incubation medium (dpm/μl). Transporter-specific uptake was obtained by subtracting the uptake into vector-transfected cells from the uptake into cDNA-transfected cells. Kinetic parameters were obtained using the following equation:

$$v = \frac{V_{max} \times S}{K_m + S} + P_{dif} \times S \quad (2)$$

where v is the uptake velocity of the substrate (pmol/min/mg protein), S is the substrate concentration in the medium (μM), K_m is the Michaelis constant (μM), V_{max} is the maximum uptake rate (pmol/min/mg protein), and P_{dif} is the nonsaturable uptake clearance (μl/min/mg protein). The Damping Gauss-Newton Method algorithm was used with a MULTI program (Yamaoka et al., 1981) to perform nonlinear least-squares data fitting. The input data were weighted as the reciprocal of the observed values. Inhibition constants (K_i) of a series of compounds could be calculated by the following equation, if the substrate concentration was low enough compared with its K_m value.

$$CL(+I) = \frac{CL}{1 + \frac{I}{K_i}} \quad (3)$$

where CL represents the uptake clearance in the absence of inhibitor, $CL(+I)$ represents the uptake clearance in the presence of inhibitor, and I represents the inhibitor concentration. When fitting the data to determine the K_i value, the input data were weighed as the reciprocal of the observed values.

To determine saturable hepatic uptake clearance in human hepatocytes, we first determined the hepatic uptake clearance ($CL_{(2\ min-0.5\ min)}$) (μl/min/10^6 cells) by calculating the slope of the uptake volume (V_d) (μl/10^6 cells) between 0.5 and 2 min as shown previously (Hirano et al., 2004) (eq. 4). The saturable component of the hepatic uptake clearance (CL_{hep}) was determined by subtracting $CL_{(2\ min-0.5\ min)}$ in the presence of 100 μM substrate (excess) from that in the presence of 0.1 μM substrate (tracer) (eq. 5).

$$CL_{(2\ min-0.5\ min)} = \frac{V_{d,2\ min} - V_{d,0.5\ min}}{2 - 0.5} \quad (4)$$

$$CL_{hep} = CL_{(2\ min-0.5\ min),tracer} - CL_{(2\ min-0.5\ min),excess} \quad (5)$$

where $CL_{(2\ min-0.5\ min),tracer}$ and $CL_{(2\ min-0.5\ min),excess}$ represent $CL_{(2\ min-0.5\ min)}$ estimated in the presence of 0.1 and 100 μM substrate, respectively.

Estimation of the Contribution of Transporters to the Hepatic Uptake in Human Hepatocytes by Western Blot Analysis. The ratio of the expression level of each transporter in human hepatocytes (per 10^6 cells) to that in the expression system (per mg protein) was calculated by the intensity of specific bands in Western blot analysis and defined as R_{exp} as shown previously (Hirano et al., 2004). The uptake clearance by each transporter in human hepatocytes was separately calculated by multiplying the uptake clearance of the pitavastatin in transporter-expressing cells (CL_{test}) by R_{exp} as described in the following equation:

$$CL_{hep,test} = CL_{test} \cdot R_{exp} \quad (6)$$

The relative contribution (percentage) of each transporter to the uptake in human hepatocytes was defined by the ratio of $CL_{hep,test}$ for target transporter to that of the sum of $CL_{hep,test}$ for OATP1B1, OATP1B3, and OATP2B1.

Prediction of Clinical DDI between Pitavastatin and Various Drugs via OATP1B1. The degree of inhibition of OATP1B1 in humans was estimated by calculating the following R values, which represent the ratio of the uptake clearance in the absence of inhibitor to that in its presence:

$$R = 1 + \frac{f_u \cdot I_{in,max}}{K_i} \quad (7)$$

where f_u represents the blood unbound fraction of the inhibitor, $I_{in,max}$ represents the estimated maximum inhibitor concentration at the inlet to the liver, and K_i was obtained in the present in vitro study using OATP1B1-expressing HEK293 cells. For the estimation of R value, $I_{in,max}$ was calculated by the method of Ito et al. (1998):

$$I_{in,max} = I_{max} + \frac{F_a \cdot Dose \cdot k_a}{Q_h} \quad (8)$$

where I_{max} represents the reported value for the maximum plasma concentration in the systemic circulation in the clinical situation, F_a represents the absorbed fraction of inhibitor, k_a is the absorption rate constant in the intestine, and Q_h represents the hepatic blood flow rate in humans (1610 ml/min). To estimate the maximum $I_{in,max}$ value, F_a was set at 1, k_a was set at 0.1 min^{-1} [minimum gastric emptying time (10 min)], and the blood-to-plasma concentration ratio was assumed to be 1, if the information from the literature was not available.

Results

Uptake of E_1S and Pitavastatin by OATP2B1-Expressing Cells. The time profiles and Eadie-Hofstee plots of the uptake of E_1S and pitavastatin by OATP2B1-expressing and vector-transfected HEK293 cells are shown in Fig. 1. Pitavastatin as well as E_1S was significantly taken up into OATP2B1-expressing HEK293 cells compared with vector-transfected cells (Fig. 1, A and B). The saturation kinetics of their uptake is shown in Fig. 1, C and D. The concentration dependence of the uptake of E_1S could be explained by a one-saturable component (Fig. 1C). The K_m and V_{max} values for the OATP2B1-mediated uptake of E_1S were 20.9 ± 2.0 μM and 1196 ± 40 pmol/min/mg protein, respectively. The nonsaturable component was observed in the Eadie-Hofstee plot even for the specific uptake of pitavastatin by OATP2B1 (Fig. 1D). The K_m and V_{max} values of pitavastatin for the saturable component and uptake clearance for the nonsaturable component were 1.17 ± 0.28 μM, 7.36 ± 1.43 pmol/min/mg protein, and 2.93 ± 0.16 μl/min/mg protein, respectively. No significant uptake of $E_2 17\beta G$ by OATP2B1 could be observed (7.51 ± 0.49 and 9.72 ± 1.29 μl/mg protein by vector-transfected and OATP2B1-expressing cells for 5 min, respectively; $n = 3$).

Western Blot Analysis of OATP2B1. The relative expression level of OATP2B1 in crude membrane from transfectants and human hepatocytes was estimated by Western blot analyses. An antiserum against OATP2B1 recognized approximately 85-kDa proteins in the crude membrane fractions prepared from human hepatocytes and OATP2B1-expressing cells (Fig. 2A). The molecular weight of OATP2B1 in human hepatocytes was almost the same as that pre-

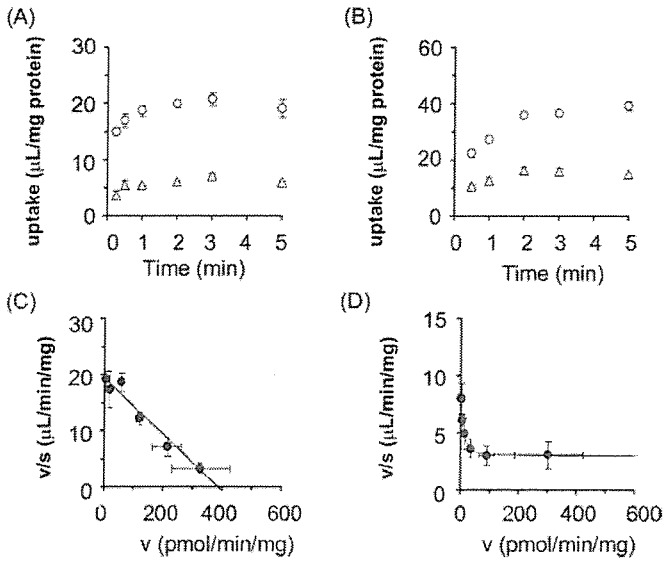

FIG. 1. Time profiles and Eadie-Hofstee plots of the uptake of [^{3}H]E_1S and [^{3}H]pitavastatin by OATP2B1-expressing HEK293 cells. The uptake of 0.1 μM [^{3}H]E_1S (A) and 0.1 μM [^{3}H]pitavastatin (B) by cDNA-transfected cells was examined at 37°C. Open circles and triangles represent the uptake in OATP2B1-expressing HEK293 cells and vector-transfected control cells, respectively. The concentration dependence of OATP2B1-mediated uptake of [^{3}H]E_1S (C) and [^{3}H]pitavastatin (D) is shown as Eadie-Hofstee plots. Closed circles represent the OATP2B1-mediated specific uptake rate, which was obtained by subtracting the initial uptake rate in vector-transfected cells from that in OATP2B1-expressing cells. The initial uptake rate calculated from the uptake of [^{3}H]E_1S and [^{3}H]pitavastatin for 1 and 2 min, respectively, was determined at various concentrations (0.3–100 μM). Solid lines represent the fitted curves obtained by nonlinear regression analysis. Each point represents the mean ± S.E. (n = 3). Where error bars are not shown, the S.E. values are within the limits of the symbol.

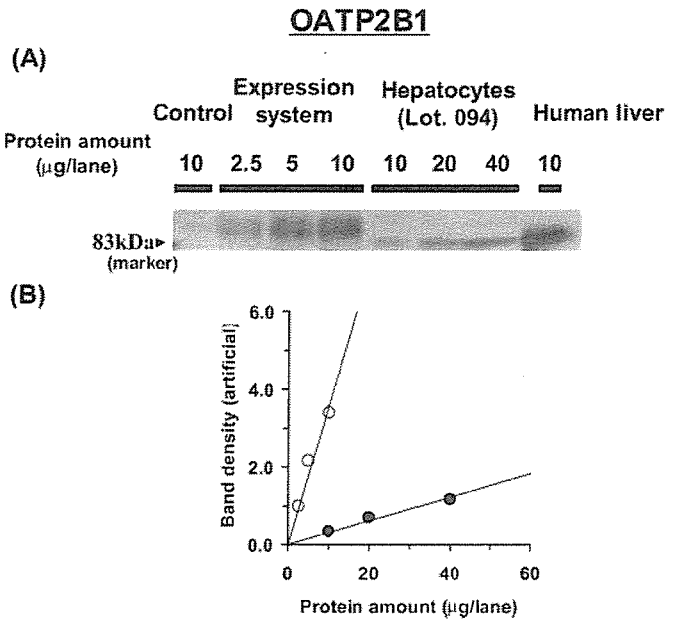

FIG. 2. Western blot analysis of OATP2B1. A, crude membrane fractions (2.5–40 μg) prepared from OATP2B1-expressed HEK293 cells and human hepatocytes (lot 094) were loaded and separated by SDS-polyacrylamide gel electrophoresis (7% separating gel). The sample designated as "Human liver" indicates that the crude membrane vesicles were prepared from a human frozen liver block (lot 020188) as a positive control. OATP2B1 was detected by preimmune antisera raised against the carboxyl terminus of human OATP2B1. B, comparison of the relative expression levels of OATP2B1 between transfectants and hepatocytes is shown. The x and y axes represent the amount of crude membrane obtained from transfectants and human hepatocytes and the intensity of the specific band in Western blot analysis, respectively. Closed circles and open circles indicate the band density of human hepatocytes (lot 094) and OATP2B1-expressing HEK293 cells, respectively. The solid lines represent the fitted lines obtained by linear regression analysis.

pared from human liver block, but was slightly lower than that in OATP2B1-expressing HEK293 cells. No specific band of OATP2B1 was detected in vector-transfected cells. Figure 2B showed the linear relationship between the applied protein amount of crude membrane obtained from OATP2B1-expressing cells and human hepatocytes and the intensity of the specific band measured by digital densitometer. The slope of the regression line in Fig. 2B reflected the relative expression level of OATP2B1 in transfectants and hepatocytes.

Estimation of Contribution of OATP1B1, OATP1B3, and OATP2B1 in Human Hepatocytes by Western Blot Analysis. We calculated the estimated uptake clearance of pitavastatin by OATP1B1, OATP1B3, and OATP2B1 in human hepatocytes by the relative expression level of each transporter (Table 1). We obtained 62.1 μg of protein in crude membrane from 1 mg of whole cell protein in OATP2B1-expressing HEK293 cells, whereas 178, 89, and 82 μg of protein were obtained in crude membrane from 10^6 human hepatocytes of lot OCF, 094, and ETR, respectively. When the band density per unit protein amount in crude membrane of OATP2B1-expressing HEK293 cells is defined as 1, the relative expression levels of OATP2B1 per unit protein amount in crude membrane of hepatocytes of lots OCF, 094, and ETR are 0.200, 0.152, and 0.112 (per microgram), respectively. Using these R_{exp} values and our previous results (Hirano et al., 2004; shown in Table 1), we estimated the relative contribution of OATP1B1, OATP1B3, and OATP2B1 to the hepatic uptake of pitavastatin in human hepatocytes.

Inhibitory Effects of $E_2$17βG and E_1S on the Uptake of Pitavastatin by Transporter-Expression System and Human Hepatocytes. Inhibitory effects of $E_2$17βG and E_1S on the uptake of pitavastatin were examined by human cryopreserved hepatocytes (Fig. 3). $E_2$17βG (100 μM) inhibited OATP1B1- and OATP1B3-mediated transport of pitavastatin to 10.0 ± 3.2 and 21.7 ± 8.7% of control, respectively (n = 3), whereas OATP2B1-mediated transport was not affected by 100 μM $E_2$17βG (91.8 ± 16.6%). In contrast, 100 μM E_1S inhibited OATP1B1- and OATP2B1-mediated transport of pitavastatin to 7.19 ± 2.94 and 56.5 ± 3.2% of control, respectively (n = 3), whereas OATP1B3-mediated transport was not affected by 100 μM E_1S (102 ± 7%). In three batches of human hepatocytes, pitavastatin uptake was almost inhibited by 100 μM $E_2$17βG (Fig. 3A) and E_1S (Fig. 3B).

Prediction of DDI between Pitavastatin and Various Compounds by OATP1B1-Expressing HEK293 Cells. To identify clinically relevant inhibitors for OATP1B1-mediated pitavastatin uptake, inhibitory effects of several compounds on the uptake of pitavastatin were determined by OATP1B1-expressing cells. These compounds include therapeutic agents that were reported to cause DDI with statins (Williams and Feely, 2002). Cyclosporin A, fenofibrate, gemfibrozil, and gemfibrozil metabolites (gemfibrozil-M3 and gemfibrozil-1-O-glucuronide) were also investigated because drug interaction studies with pitavastatin have been previously reported (Hasunuma et al., 2003; Mathew et al., 2004). Most of the compounds we tested could inhibit OATP1B1-mediated pitavastatin uptake (Table 2). We also obtained the blood unbound fraction (f_u) and calculated the estimated maximum concentration at the inlet to the liver ($I_{in,max}$) of the inhibitors from the literature information (Clark et al., 1992; Hardman et al., 2001; package insert of each drug). Inhibition constants (K_i) of various compounds for OATP1B1 obtained in the present study and the ratio of the uptake clearance in the absence of inhibitor to that in its presence (R value) are summarized in Table 2. R values of cyclosporin A, rifampicin, rifamycin SV, clarithromycin,

TABLE 1

Contribution of OATP1B1, OATP1B3, and OATP2B1 to the hepatic uptake of pitavastatin determined by the relative expression level

Hepatocyte Lot	Ratio of Expression Level[a] (Hepatocyte/Expression System)			Estimated Clearance[b]		
	$R_{exp,OATP1B1}$	$R_{exp,OATP1B3}$	$R_{exp,OATP2B1}$	OATP1B1	OATP1B3	OATP2B1
					μl/min/10⁶ cells	
OCF	2.90[c]	1.21[c]	0.200	222	37.0	0.658
				85.5%	14.3%	0.253%
094	1.58[c]	0.930[c]	0.152	121	28.5	0.500
				80.7%	19.0%	0.333%
ETR	0.890[c]	0.737[c]	0.112	68.2	22.6	0.368
				74.8%	24.8%	0.405%

[a] Ratio of the expression level was determined by the intensity of the specific band in the crude membrane prepared from human hepatocytes (per 10^6 cells) divided by that in the crude membrane from transporter-expressing cells (per milligram) in Western blot analysis.

[b] In the 'Estimated Clearance' column, each percentage value indicates the percentage of the OATP1B1-, OATP1B3-, or OATP2B1-mediated uptake clearance relative to the sum of the estimated clearance mediated by OATP1B1, OATP1B3, and OATP2B1. The details of this estimation are described under *Materials and Methods*.

[c] Values from Hirano et al. (2004).

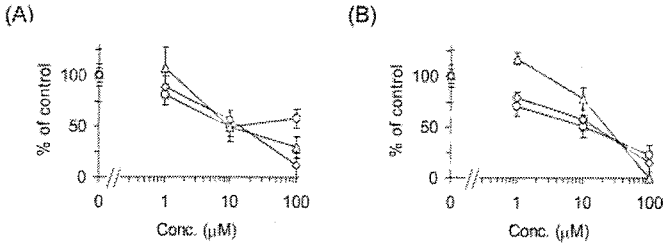

FIG. 3. Inhibitory effects of $E_2 17\beta G$ and $E_1 S$ on the uptake of [^{3}H]pitavastatin by human hepatocytes. The transport of [^{3}H]pitavastatin (0.1 μM) into human hepatocytes was determined in the presence or absence of $E_2 17\beta G$ (A) and $E_1 S$ (B) at the designated concentrations. Open circles, triangles, and squares represent the uptake in human hepatocytes of lots OCF, 094, and ETR, respectively. The detailed method for calculation of the uptake clearance in hepatocytes (CL_{hep}) is described under *Materials and Methods*. The values are expressed as a percentage of the uptake of [^{3}H]pitavastatin in the absence of inhibitors. Each point represents the mean ± S.E. (n = 3).

and indinavir were higher than 2.5, suggesting that these drugs can interact with pitavastatin in a clinical situation.

Inhibitory Effects of Cyclosporin A, Gemfibrozil, and Its Metabolites on the Transcellular Transport of Pitavastatin in OATP1B1/MRP2, OATP1B1/MDR1, and OATP1B1/BCRP Double Transfectants. The inhibitory effects of cyclosporin A, gemfibrozil, gemfibrozil-1-*O*-glucuronide, and gemfibrozil-M3 on the transcellular transport of pitavastatin were investigated in double-transfected cells. The transcellular transport clearance (PS_{net}) of pitavastatin was drastically decreased by cyclosporin A in all kinds of double transfectants (Fig. 4A). The efflux clearance from cells to the apical compartment (PS_{apical}) was also potently reduced by cyclosporin A (Fig. 5A). In contrast, gemfibrozil and gemfibrozil-1-*O*-glucuronide did not change either PS_{net} or PS_{apical} up to 100 μM (Figs. 4 and 5). Gemfibrozil-M3 (300 μM) could not inhibit the PS_{apical} of pitavastatin in OATP1B1/BCRP-, OATP1B1/MDR1-, and OATP1B1/MRP2-expressing MDCKII cells (data not shown). The K_i values of these inhibitors on the PS_{net} and PS_{apical} of pitavastatin are summarized in Table 3.

TABLE 2

The K_i values for OATP1B1-mediated pitavastatin uptake and the prediction of the possibility of DDI by considering the maximum plasma unbound concentration at the inlet to the liver

The K_i values are expressed as mean ± computer-calculated S.D. R value = $1 + f_u \cdot I_{in,max}/K_i$.

Inhibitor	K_i Value for OATP1B1	R Value
	μM	
Cyclosporin A	0.242 ± 0.029	3.55
Tacrolimus	0.611 ± 0.069	1.20
Rifampicin	0.477 ± 0.030	13.4
Rifamycin SV	0.171 ± 0.024	65.6
Tolbutamide	>100	<1.21
Glibenclamide	0.746 ± 0.101	1.00
Fluconazole	>100	<1.25
Ketoconazole	19.2 ± 3.9	1.03
Itraconazole	>100	<1.00
Gemfibrozil	25.2 ± 4.7	1.08
Gemfibrozil-1-*O*-glucuronide	22.6 ± 5.8	1.10[a]
Gemfibrozil-M3	>300	<1.03[a]
Clofibrate	>300	<1.03
Ciprofibrate	141 ± 22	1.01
Bezafibrate	68.6 ± 11.9	1.03
Fenofibrate	>300	<1.00
Cimetidine	>300	<1.14
Ranitidine	>300	<1.16
Valsartan	8.96 ± 1.33	1.10
Telmisartan	0.436 ± 0.043	1.16
Chlorzoxazone	>100	<1.00
Colchichine	>100	<1.07
Phenytoin	>100	<1.03
Clarithromycin	8.26 ± 0.54	3.29
Erythromycin	11.4 ± 2.1	1.25
Indinavir	18.4 ± 1.9	2.77
Ritonavir	0.781 ± 0.048	2.25
Saquinavir	1.59 ± 0.13	1.62
Probenecid	76.2 ± 7.1	1.85
Methotrexate	>300	<1.01
Digoxin	31.7 ± 3.0	1.00
Diltiazem	>100	<1.03
Verapamil	51.6 ± 15.9	1.02
Warfarin	83.3 ± 9.7	1.00

[a] These values were calculated by using the reported values for the maximum plasma concentration of inhibitors in the clinical situations, instead of $I_{in,max}$, because we did not have enough parameters to estimate the $I_{in,max}$ value.

Discussion

In the present study, we have excluded the possibility of a major contribution of OATP2B1 to the hepatic uptake of pitavastatin and confirmed that OATP1B1 is the most important transporter for its uptake. Next, the inhibitory effects of pitavastatin uptake by several drugs in OATP1B1-expressing cells were also investigated, and we discussed the possibility of DDI in clinical stage by considering the inhibition constant (K_i) obtained from in vitro analysis and the estimated maximum unbound concentration of each inhibitor at the inlet to the liver.

We observed the significant saturable uptake of pitavastatin in OATP2B1-expressing cells compared with control cells at pH 7.4 with a K_m value of 1.17 μM (Fig. 1). It has been shown that specific uptake of pravastatin by OATP2B1 was not significantly observed at pH 7.4, whereas it can be transported at pH 5.0 (Nozawa et al., 2004), indicating that pitavastatin is preferentially recognized by OATP2B1

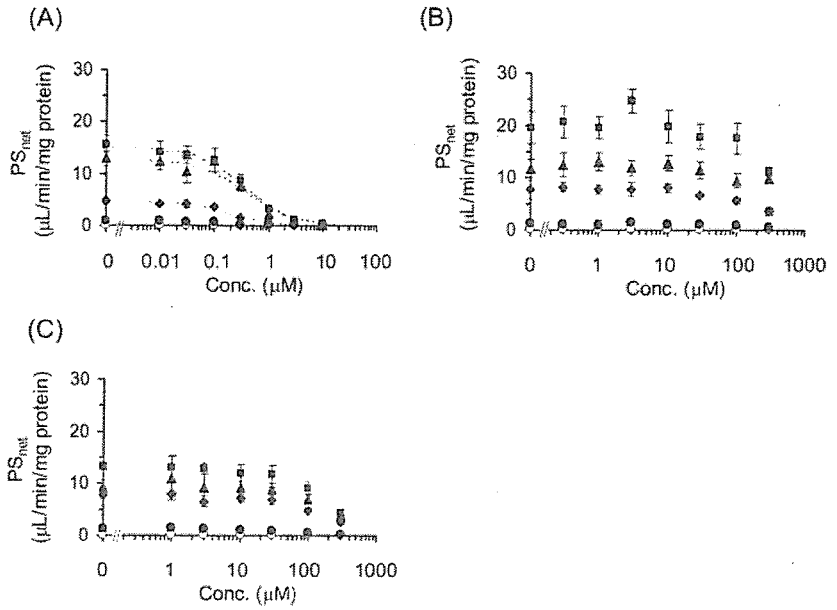

FIG. 4. Inhibitory effects of cyclosporin A, gemfibrozil, and gemfibrozil-1-*O*-glucuronide on the transcellular transport of [^{3}H]pitavastatin. The basal-to-apical flux of [^{3}H]pitavastatin (0.3 μM) across MDCKII monolayer expressing OATP1B1 (closed circles), OATP1B1/BCRP (closed diamonds), OATP1B1/MDR1 (closed squares), and OATP1B1/MRP2 (closed triangles) was determined compared with vector-transfected control cells (open circles) in the absence and presence of cyclosporin A (A), gemfibrozil (B), or gemfibrozil-1-*O*-glucuronide (C). The *x* and *y* axes represent the concentration of each inhibitor in the medium at the basal compartment and the transport clearance for the transcellular transport (PS_{net}) of [^{3}H]pitavastatin (μl/min/mg protein). Each point and vertical bar represent the mean ± S.E. of three determinations. Where vertical bars are not shown, the S.E. values are within the limits of the symbol. Dotted lines represent the fitted curves obtained by nonlinear regression analysis.

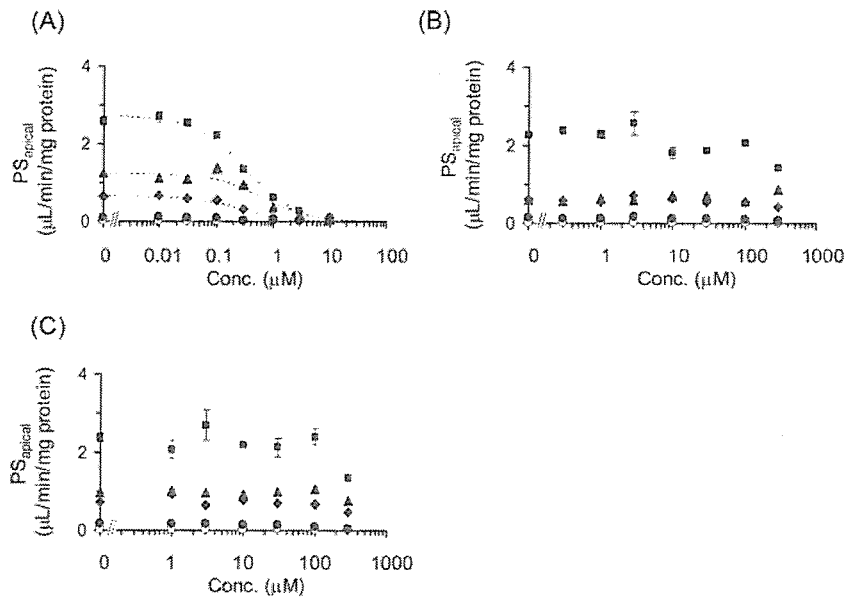

FIG. 5. Inhibitory effects of cyclosporin A, gemfibrozil, and gemfibrozil-1-*O*-glucuronide on the efflux transport of [^{3}H]pitavastatin across the apical membrane of MDCKII cells. The efflux transport clearance of [^{3}H]pitavastatin (0.3 μM) across the apical membrane (PS_{apical}) of MDCKII monolayer expressing OATP1B1 (closed circles), OATP1B1/BCRP (closed diamonds), OATP1B1/MDR1 (closed squares), and OATP1B1/MRP2 (closed triangles) was determined compared with vector-transfected control cells (open circles) in the absence and presence of cyclosporin A (A), gemfibrozil (B), or gemfibrozil-1-*O*-glucuronide (C). The *x* and *y* axes represent the concentration of each inhibitor in the medium at the basal compartment and the transport clearance for the efflux transport across the apical membrane (PS_{apical}) of [^{3}H]pitavastatin (μl/min/mg protein). Each point and vertical bar represents the mean ± S.E. of three determinations. Where vertical bars are not shown, the S.E. values are within the limits of the symbol. Dotted lines represent the fitted curves obtained by nonlinear regression analysis.

compared with pravastatin. The K_m value of E_1S for OATP2B1 from our analyses was 20.9 μM (Fig. 1), which was almost comparable to the reported values (Kullak-Ublick et al., 2001; Nozawa et al., 2004), whereas the significant uptake of $E_2 17\beta G$ at pH 7.4 was not detected as described previously (Kullak-Ublick et al., 2001; Nozawa et al., 2004).

Then, to refute the possibility that OATP2B1 plays an important role in the pitavastatin uptake in human hepatocytes and confirm the major contribution of OATP1B1, we took two strategies: 1) to check the inhibitable portion of pitavastatin uptake by two inhibitors in human hepatocytes, and 2) to compare the relative expression level of OATP2B1 in human hepatocytes and OATP2B1-expressing cells by Western blot analysis. As a result of the first approach, pitavastatin uptake in human hepatocytes was almost completely suppressed

TABLE 3

The K_i values of cyclosporin A, gemfibrozil, and gemfibrozil-1-O-glucuronide for the PS_{net} and PS_{apical} of pitavastatin in double-transfected cells

The values are expressed as mean ± computer-calculated S.D.

Transfectants	Cyclosporin A	Gemfibrozil	Gemfibrozil-1-*O*-glucuronide
PS_{net} (K_i, μM)			
OATP1B1/BCRP	0.194 ± 0.048	>100	>100
OATP1B1/MDR1	0.359 ± 0.046	>100	>100
OATP1B1/MRP2	0.407 ± 0.132	>100	>100
PS_{apical} (K_i, μM)			
OATP1B1/BCRP	0.273 ± 0.083	>300	>300
OATP1B1/MDR1	0.330 ± 0.037	>300	>300
OATP1B1/MRP2	0.662 ± 0.252	>300	>300

by both 100 μM $E_2$17βG (inhibitor of OATP1B1/OATP1B3) and E_1S (inhibitor of OATP1B1/OATP2B1) (Fig. 3), suggesting that OATP1B1 mainly contributes to the hepatic uptake of pitavastatin. In contrast, the uptake of telmisartan, which can be accepted by OATP1B3, but not OATP1B1, into human hepatocytes could not be inhibited by 100 μM E_1S (Ishiguro et al., 2006), supporting the validity of our approach. Moreover, from the comparison of the expression level of OATP2B1 between transfectants and hepatocytes by Western blot analysis (Fig. 2), we could calculate the OATP1B1-, OATP1B3-, and OATP2B1-mediated uptake into hepatocytes by multiplying the uptake clearance of pitavastatin in the expression system by the ratio of the expression level in these cells (R_{exp}). The results indicated that the contribution of OATP2B1 to the hepatic uptake of pitavastatin was less than 1%, although it is a substrate of OATP2B1, and that OATP1B1 is the most important in the hepatic uptake of pitavastatin, which is consistent with the previous results calculated from other approaches (Hirano et al., 2004).

Pitavastatin is mainly eliminated from liver in an unchanged form (Kojima et al., 2001). From the pharmacokinetic point of view, the change in the hepatic uptake clearance always directly affects the overall hepatic clearance for this type of drug (Shitara et al., 2005). Since we clarified that pitavastatin is taken up into the hepatocytes mainly by OATP1B1 in the present study, we focused on the inhibitory effects of various drugs on the OATP1B1-mediated uptake of pitavastatin. The combination therapy of statins and various drugs, such as fibrates, immune suppressants, antidiabetic drugs, antihypertensive drugs, and antibiotics, is widely used in the clinical situation (Williams and Feely, 2002). It has been reported that the plasma area under the plasma concentration-time curve of several statins was increased by coadministration of cyclosporin A and gemfibrozil (Shitara et al., 2005). Recently, Shitara et al. (2003) have demonstrated that inhibition of OATP1B1 is a major mechanism of DDI between cerivastatin and cyclosporin A. Campbell et al. (2004) also suggested that unconjugated hyperbilirubinemia induced by indinavir, rifamycin SV, and cyclosporin A is partly caused by the inhibition of OATP1B1-mediated uptake. Although pitavastatin uptake could be inhibited by several drugs in in vitro experiments, from the results of our calculation (Ito et al., 1998), the R values of most of the drugs we tested are almost equal to 1 (Table 2). To avoid the false-negative prediction of DDI, we estimated the inhibitory effects of the maximum plasma unbound concentration of inhibitors at the inlet to the liver ($I_{in,max}$). Therefore, it is unlikely that the OATP1B1-mediated DDI between pitavastatin and these drugs occurs in the clinical stage. However, we should pay attention to the OATP1B1-mediated DDI for pitavastatin with coadministration of cyclosporin A, rifampicin, rifamycin SV, clarithromycin, and indinavir because their R values exceeded 2.5 (Table 2), although the degree of the inhibition could be overestimated. We should notice that these drugs may also cause DDI with compounds that are mainly eliminated from liver via OATP1B1, including other statins. The previous clinical studies have shown that plasma concentration of pitavastatin was increased by cyclosporin A (Hasunuma et al., 2003), but not gemfibrozil and fenofibrate (Mathew et al., 2004). This evidence was consistent with our prediction (Table 2).

Conversely, gemfibrozil caused an increase in plasma concentration of cerivastatin (Backman et al., 2002). One of the major mechanisms of DDI between cerivastatin and gemfibrozil was considered to be the inhibition of CYP2C8-mediated metabolism of cerivastatin by gemfibrozil-1-*O*-glucuronide, which is thought to be concentrated in hepatocytes (Shitara et al., 2004). Gemfibrozil is metabolized into M3 and its glucuronide in the liver. Therefore, to investigate whether gemfibrozil, gemfibrozil-M3, and gemfibrozil-1-*O*-glucuronide could affect the transcellular transport by the inhibition of efflux transporter in liver, we checked their inhibitory effects on transcellular transport clearance (PS_{net}) and efflux clearance (PS_{apical}) in double-transfected cells. As a result, gemfibrozil and its metabolites could not inhibit the efflux transporters and affect transcellular transport, whereas cyclosporin A strongly inhibited both PS_{net} and PS_{apical} in all kinds of double-transfected cells (Figs. 4 and 5). This result suggested that the DDI between cyclosporin A and pitavastatin may be caused not only by the inhibition of OATP1B1-mediated uptake, but also by the inhibition of efflux transport mediated by MRP2, MDR1, and BCRP.

In conclusion, we have confirmed the major contribution of OATP1B1 to the hepatic uptake of pitavastatin in human hepatocytes. In addition, focusing on OATP1B1, inhibitory effects of various drugs on pitavastatin uptake were determined by OATP1B1-expressing cells, and its clinical relevance was discussed by considering the R values. Our results suggested that OATP1B1-mediated DDI between pitavastatin and some drugs indicated above may be clinically relevant and should be taken notice of during coadministration of inhibitors of OATP1B1.

Acknowledgments. We thank Dr. Piet Borst (The Netherlands Cancer Institutes, Amsterdam, The Netherlands) for providing the MDCKII cells expressing MRP2 and MDR1, Dr. Yoshihiro Miwa (University of Tsukuba, Japan) for providing pEB6CAGMCS/SRZeo vector, and Ying Tian and Miyuki Kambara for the construction of OATP2B1-expressing cells. We also thank Kowa Co. Ltd. (Tokyo, Japan) for providing radiolabeled pitavastatin and unlabeled pitavastatin, and Sankyo Co., Ltd. (Tokyo, Japan) and Chemtech Labo. Inc. (Tokyo, Japan) for providing gemfibrozil-1-*O*-glucuronide.

References

Aoki T, Nishimura H, Nakagawa S, Kojima J, Suzuki H, Tamaki T, Wada Y, Yokoo N, Sato F, Kimata H, et al. (1997) Pharmacological profile of a novel synthetic inhibitor of 3-hydroxy-3-methylglutaryl-coenzyme A reductase. *Arzneim-Forsch* **47**:904–909.

Backman JT, Kyrklund C, Neuvonen M, and Neuvonen PJ (2002) Gemfibrozil greatly increases plasma concentrations of cerivastatin. *Clin Pharmacol Ther* **72**:685–691.

Campbell SD, de Morais SM, and Xu JJ (2004) Inhibition of human organic anion transporting polypeptide OATP1B1 as a mechanism of drug-induced hyperbilirubinemia. *Chem-Biol Interact* **150**:179–187.

Clark WG, Brater DC, Johnson AR, and Goth A (1992) *Goth's Medical Pharmacology*, 13th ed, Mosby-Year Book, St. Louis.

Evans M and Rees A (2002) Effects of HMG-CoA reductase inhibitors on skeletal muscle: are all statins the same? *Drug Saf* **25**:649–663.

Hagenbuch B and Meier PJ (2003) The superfamily of organic anion transporting polypeptides. *Biochim Biophys Acta* **1609**:1–18.

Hardman J, Limbird L, and Gilman AG (2001) *Goodman and Gilman's The Pharmacological Basis of Therapeutics*, 9th ed, McGraw-Hill, New York.

Hasunuma T, Nakamura M, Yachi T, Arisawa N, Fukushima K, Iijima H, and Saito Y (2003) The drug-drug interactions of pitavastatin (NK-104), a novel HMG-CoA reductase inhibitor and cyclosporine. *J Clin Ther Med* **19**:381–389.

Hirano M, Maeda K, Shitara Y, and Sugiyama Y (2004) Contribution of OATP2 (OATP1B1) and OATP8 (OATP1B3) to the hepatic uptake of pitavastatin in humans. *J Pharmacol Exp Ther* **311**:139–146.

Ichimaru N, Takahara S, Kokado Y, Wang JD, Hatori M, Kameoka H, Inoue T, and Okuyama A (2001) Changes in lipid metabolism and effect of simvastatin in renal transplant recipients induced by cyclosporine or tacrolimus. *Atherosclerosis* **158**:417–423.

Ishiguro N, Maeda K, Kishimoto W, Saito A, Harada A, Ebner T, Roth W, Igarashi T, and Sugiyama Y (2006) Predominant contribution of OATP1B3 to the hepatic uptake of telmisartan, an angiotensin II receptor antagonist, in humans. *Drug Metab Dispos* **34:**1109–1115.

Ito K, Iwatsubo T, Kanamitsu S, Ueda K, Suzuki H, and Sugiyama Y (1998) Prediction of pharmacokinetic alterations caused by drug-drug interactions: metabolic interaction in the liver. *Pharmacol Rev* **50:**387–412.

Kajinami K, Takekoshi N, and Saito Y (2003) Pitavastatin: efficacy and safety profiles of a novel synthetic HMG-CoA reductase inhibitor. *Cardiovasc Drug Rev* **21:**199–215.

Kantola T, Kivisto KT, and Neuvonen PJ (1998) Erythromycin and verapamil considerably increase serum simvastatin and simvastatin acid concentrations. *Clin Pharmacol Ther* **64:**177–182.

Kimata H, Fujino H, Koide T, Yamada Y, Tsunenari Y, Yonemitsu M, and Yanagawa Y (1998) Studies on the metabolic fate of NK-104, a new inhibitor of HMG-CoA reductase: I. Absorption, distribution, metabolism and excretion in rats. *Xenobiol Metab Dispos* **13:**484–498.

Kobayashi D, Nozawa T, Imai K, Nezu J, Tsuji A, and Tamai I (2003) Involvement of human organic anion transporting polypeptide OATP-B (SLC21A9) in pH-dependent transport across intestinal apical membrane. *J Pharmacol Exp Ther* **306:**703–708.

Kojima J, Ohshima T, Yoneda M, and Sawada H (2001) Effect of biliary excretion on the pharmacokinetics of pitavastatin (NK-104) in dogs. *Xenobio Metab Dispos* **16:**497–502.

Kullak-Ublick GA, Ismair MG, Stieger B, Landmann L, Huber R, Pizzagalli F, Fattinger K, Meier PJ, and Hagenbuch B (2001) Organic anion-transporting polypeptide B (OATP-B) and its functional comparison with three other OATPs of human liver. *Gastroenterology* **120:**525–533.

Lowry OH, Rosebrough NJ, Farr AL, and Randall RJ (1951) Protein measurement with the Folin phenol reagent. *J Biol Chem* **193:**265–267

Mathew P, Cuddy T, Tracewell WG, and Salazar D (2004) An open-label study on the pharmacokinetics (PK) of pitavastatin (NK-104) when administered concomitantly with fenofibrate or gemfibrozil in healthy volunteers. *Clin Pharmacol Ther* **75:**33.

Matsushima S, Maeda K, Kondo C, Hirano M, Sasaki M, Suzuki H, and Sugiyama Y (2005) Identification of the hepatic efflux transporters of organic anions using double transfected MDCKII cells expressing human OATP1B1/MRP2, OATP1B1/MDR1 and OATP1B1/BCRP. *J Pharmacol Exp Ther* **314:**1059–1067.

Mizuno N, Niwa T, Yotsumoto Y, and Sugiyama Y (2003) Impact of drug transporter studies on drug discovery and development. *Pharmacol Rev* **55:**425–461.

Neuvonen PJ, Kantola T, and Kivisto KT (1998) Simvastatin but not pravastatin is very susceptible to interaction with the CYP3A4 inhibitor itraconazole. *Clin Pharmacol Ther* **63:**332–341.

Nozawa T, Imai K, Nezu J, Tsuji A, and Tamai I (2004) Functional characterization of pH-sensitive organic anion transporting polypeptide OATP-B in human. *J Pharmacol Exp Ther* **308:**438–445.

Olbricht C, Wanner C, Eisenhauer T, Kliem V, Doll R, Boddaert M, O'Grady P, Krekler M, Mangold B, and Christians U (1997) Accumulation of lovastatin, but not pravastatin, in the blood of cyclosporine-treated kidney graft patients after multiple doses. *Clin Pharmacol Ther* **62:**311–321.

Sasaki M, Suzuki H, Ito K, Abe T, and Sugiyama Y (2002) Transcellular transport of organic anions across a double-transfected Madin-Darby canine kidney II cell monolayer expressing both human organic anion-transporting polypeptide (OATP2/SLC21A6) and Multidrug resistance-associated protein 2 (MRP2/ABCC2). *J Biol Chem* **277:**6497–6503.

Shimizu M, Fuse K, Okudaira K, Nishigaki R, Maeda K, Kusuhara H, and Sugiyama Y (2005) Contribution of OATP (organic anion-transporting polypeptide) family transporters to the hepatic uptake of fexofenadine in humans. *Drug Metab Dispos* **33:**1477–1481.

Shitara Y, Hirano M, Sato H, and Sugiyama Y (2004) Gemfibrozil and its glucuronide inhibit the organic anion transporting polypeptide 2 (OATP2/OATP1B1:SLC21A6)-mediated hepatic uptake and CYP2C8-mediated metabolism of cerivastatin: analysis of the mechanism of the clinically relevant drug-drug interaction between cerivastatin and gemfibrozil. *J Pharmacol Exp Ther* **311:**228–236.

Shitara Y, Itoh T, Sato H, Li AP, and Sugiyama Y (2003) Inhibition of transporter-mediated hepatic uptake as a mechanism for drug-drug interaction between cerivastatin and cyclosporin A. *J Pharmacol Exp Ther* **304:**610–616.

Shitara Y, Sato H, and Sugiyama Y (2005) Evaluation of drug-drug interaction in the hepatobiliary and renal transport of drugs. *Annu Rev Pharmacol Toxicol* **45:**689–723.

Simonson SG, Raza A, Martin PD, Mitchell PD, Jarcho JA, Brown CD, Windass AS, and Schneck DW (2004) Rosuvastatin pharmacokinetics in heart transplant recipients administered an antirejection regimen including cyclosporine. *Clin Pharmacol Ther* **76:**167–177.

Sugiyama D, Kusuhara H, Shitara Y, Abe T, Meier PJ, Sekine T, Endou H, Suzuki H, and Sugiyama Y (2001) Characterization of the efflux transport of 17beta-estradiol-D-17beta-glucuronide from the brain across the blood-brain barrier. *J Pharmacol Exp Ther* **298:**316–322.

Tamai I, Nozawa T, Koshida M, Nezu J, Sai Y, and Tsuji A (2001) Functional characterization of human organic anion transporting polypeptide B (OATP-B) in comparison with liver-specific OATP-C. *Pharm Res (NY)* **18:**1262–1269.

Williams D and Feely J (2002) Pharmacokinetic-pharmacodynamic drug interactions with HMG-CoA reductase inhibitors. *Clin Pharmacokinet* **41:**343–370.

Yamaoka K, Tanigawara Y, Nakagawa T, and Uno T (1981) A pharmacokinetic analysis program (MULTI) for microcomputer. *J Pharmacobio-Dyn* **4:**879–885.

Address correspondence to: Dr. Yuichi Sugiyama, Department of Molecular Pharmacokinetics, Graduate School of Pharmaceutical Sciences, The University of Tokyo, 7-3-1 Hongo, Bunkyo-ku, Tokyo, 113-0033 Japan. E-mail: sugiyama@mol.f.u-tokyo.ac.jp

0090-9556/06/3407-1109–1115$20.00
DRUG METABOLISM AND DISPOSITION

DMD 34:1109–1115, 2006

Vol. 34, No. 7
9175/3119866
Printed in U.S.A.

PREDOMINANT CONTRIBUTION OF OATP1B3 TO THE HEPATIC UPTAKE OF TELMISARTAN, AN ANGIOTENSIN II RECEPTOR ANTAGONIST, IN HUMANS

Naoki Ishiguro, Kazuya Maeda, Wataru Kishimoto, Asami Saito, Akiko Harada, Thomas Ebner, Willy Roth, Takashi Igarashi, and Yuichi Sugiyama

Department of Pharmacokinetics and Non-Clinical Safety, Kawanishi Pharma Research Institute, Nippon Boehringer Ingelheim Co., Ltd., Hyogo, Japan (N.I., W.K., A.S., A.H., T.I.); Department of Molecular Pharmacokinetics, Graduate School of Pharmaceutical Sciences, the University of Tokyo, Tokyo, Japan (K.M., Y.S.); and Department of Pharmacokinetics and Drug Metabolism, Boehringer Ingelheim Pharma KG, Biberach on der Riss, Germany (T.E., W.R.)

ABSTRACT:

Telmisartan, a nonpeptide angiotensin II receptor antagonist, is selectively distributed to liver. In the present study, we have characterized the contribution of organic anion transporting polypeptide (OATP) isoforms to the hepatic uptake of telmisartan by isolated rat hepatocytes, human cryopreserved hepatocytes, and human transporter-expressing cells. Because it is difficult to evaluate the transport activity of telmisartan because of its extensive adsorption to cells and culture materials, we performed the uptake study in the presence of human serum albumin. The saturable uptake of telmisartan into isolated rat hepatocytes took place in a Na^+-independent manner and was inhibited by pravastatin, taurocholate, and digoxin, which are Oatp substrates and inhibitors, but not by organic cation, tetraethylammonium, indicating the involvement of Oatp isoforms in its uptake into rat hepatocytes. To identify which human OATP transporters are important for the hepatic uptake of telmisartan, the uptake assay was carried out using OATP1B1- and OATP1B3-expressing human embryonic kidney 293 cells and cryopreserved human hepatocytes. The uptake of telmisartan by OATP1B3-expressing cells was saturable (K_m = 0.81 μM) and significantly higher than that by vector-transfected cells. In contrast, no significant uptake was observed in OATP1B1-expressing cells. We also observed the saturable uptake of telmisartan by human hepatocytes. Thirty micromolar estrone-3-sulfate, which can selectively inhibit OATP1B1-mediated uptake compared with OATP1B3, did not inhibit the uptake of telmisartan in human hepatocytes, whereas it could inhibit the uptake of estradiol 17β-D-glucuronide mediated by OATP1B1. These results suggest that OATP1B3 is predominantly involved in the hepatic uptake of telmisartan in humans.

The renin-angiotensin-aldosterone system plays a central role in blood pressure regulation (Hedner, 1999). This system leads to the production of the hormone angiotensin I, which is converted to the active hormone angiotensin II by angiotensin-converting enzyme. Angiotensin II receptor antagonists prevent angiotensin II from exerting its vasoconstrictive effects on blood vessels (Oliverio and Coffman, 1997). Five nonpeptide angiotensin receptor antagonists, losartan, candesartan cilexetil, valsartan, telmisartan, and olmesartan medoxomil, are commercially available in Japan. Losartan, candesartan cilexetil, and olmesartan medoxomil are prodrugs, whereas valsartan and telmisartan are themselves pharmacologically active. All of them are mainly excreted into feces from the liver.

Telmisartan (Fig. 1) is a lipophilic compound with a log *P* value of 3.2, and it exists in anionic form at neutral pH (Wienen et al., 2000). Telmisartan is metabolized to an inactive acylglucuronide conjugate by UDP-glucuronosyltransferases in the intestinal wall and liver (Stangier et al., 2000c). The acylglucuronide is rapidly excreted into the bile and accounts for 10% of the circulating drug-related material 1 h after p.o. administration of telmisartan (Stangier et al., 2000a,c). Telmisartan is selectively distributed to the liver in rats with a liver/plasma concentration ratio of more than 40 (Wienen et al., 2000). After a single p.o. and i.v. administration in humans, more than 98% of the total radioactivity was recovered in feces as a parent drug, and less than 1% of the radioactivity was recovered in urine (Stangier et al., 2000a). Telmisartan shows a large interindividual variability in its plasma concentrations, and both the maximum concentration in plasma (C_{max}) and area under the plasma concentration-time curve (AUC) increased in a slightly more than the dose-proportional manner after p.o. administration (Stangier et al., 2000a,c). Because liver is a major clearance organ of telmisartan, it is essential to assess the uptake mechanism of telmisartan by human hepatocytes to gain an insight into the mechanism for its nonlinear pharmacokinetics and large interindividual variability.

Several transporters, such as Na^+-taurocholate cotransporting polypeptide and organic anion transporting polypeptide (OATP) 1B1 (previously called OATP-C/OATP2/LST-1), OATP1B3 (previously called OATP8/LST-2), OATP2B1 (previously called OATP-B), organic anion transporter 2, and organic cation transporter 1, are ex-

This work was supported in part by a Health and Labor Sciences Research Grants from Ministry of Health, Labor, and Welfare for the Research on Advanced Medical Technology and Grant-in Aid for Young Scientists (B) (17790113) from the Ministry of Education, Culture, Sports, Science, and Technology.

Article, publication date, and citation information can be found at http://dmd.aspetjournals.org.

doi:10.1124/dmd.105.009175.

ABBREVIATIONS: AUC, area under the plasma concentration-time curve; OATP, organic anion transporting polypeptide; $E_2$17βG, estradiol 17β-D-glucuronide; CCK-8, cholecystokinin octapeptide; E-sul, estrone-3-sulfate; TEA, tetraethylammonium; HEK, human embryonic kidney; HSA, human serum albumin.

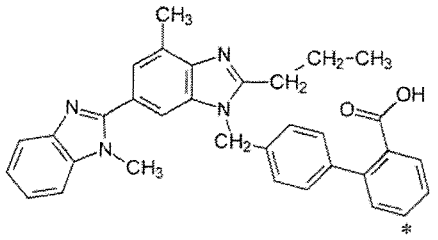

FIG. 1. Chemical structure of [^{3}H]telmisartan. The asterisk denotes the position of the ^{3}H-label.

pressed on the sinusoidal membrane of hepatocytes and are thought to be involved in the transport of a wide variety of compounds including clinically used drugs, such as 3-hydroxy-3-methylglutaryl CoA reductase inhibitors (statins), from blood into hepatocytes (Abe et al., 1999; Hsiang et al., 1999; Kok et al., 2000; Konig et al., 2000a,b; Tamai et al., 2000; Faber et al., 2003; Hirano et al., 2004). In particular, OATP1B1 and OATP1B3 are mainly expressed in human liver (Hagenbuch and Meier, 2003), and the substrate specificity of OATP1B3 commonly overlaps that of OATP1B1, so several compounds can be bisubstrates of both OATP1B1 and OATP1B3, such as estradiol 17β-D-glucuronide ($E_2$17βG), pitavastatin, and rifampicin (Vavricka et al., 2002; Hirano et al., 2004). Hirano et al. (2004) have recently established methods for estimating the contribution of OATP1B1 and OATP1B3 to the hepatic uptake of a number of compounds. They have shown that pitavastatin and $E_2$17βG are taken up in human hepatocytes mainly by OATP1B1. On the other hand, the uptake of fexofenadine, an H_1 receptor antagonist, was mainly mediated by OATP1B3 rather than OATP1B1 (Shimizu et al., 2005). This kind of information is helpful for predicting the effect of changes in expression level and function of certain transporters caused by genetic polymorphisms, pathophysiological conditions, and transporter-mediated drug-drug interactions on the overall hepatic uptake clearance and subsequent pharmacokinetics of drugs. Moreover, if compounds can selectively inhibit OATP1B1- or OATP1B3-mediated transport, we can also easily calculate the contribution of each transporter to the uptake of particular compounds in human hepatocytes by estimating the fraction of their uptake that can be inhibited by transporter-selective inhibitors. However, our preliminary study and a previous report showed that cholecystokinin octapeptide (CCK-8) could also inhibit OATP1B1-mediated transport (Nozawa et al., 2003), indicating that it cannot be used as an OATP1B3-selective inhibitor, although it is selectively transported by OATP1B3 (Ismair et al., 2001). On the other hand, there is little information about selective inhibitors against OATP1B1.

Therefore, the aim of our study is to show the involvement of OATP family transporters in the hepatic uptake process of telmisartan and estimate the contribution of OATP1B1 and OATP1B3 to its uptake in human hepatocytes by a newly developed estimation method using the OATP1B1-selective inhibitor estrone-3-sulfate (E-sul).

Materials and Methods

Chemicals. [^{3}H]Telmisartan (762 GBq/mmol, radiochemical purity >98%), 4′-[(1,4′-dimethyl-2′-propyl[2,6′-bi-1*H*-benzimidazol]-1′-yl)methyl]-[1,1′-biphenyl]-2-carboxylic acid, and unlabeled telmisartan were synthesized by Boehringer Ingelheim Pharma KG (Biberach, Germany) (Ries et al., 1993). [^{3}H]$E_2$17βG, [^{3}H]E-sul, and [^{3}H]taurocholate were purchased from PerkinElmer Life and Analytical Sciences (Boston, MA). [^{3}H]CCK-8 was purchased from Amersham Biosciences UK Ltd. (Little Chalfont, Buckinghamshire, UK). Unlabeled $E_2$17βG, E-sul, taurocholate, CCK-8, and digoxin were purchased from Sigma-Aldrich (St. Louis, MO). Pravastatin and tetraethylammonium (TEA) were obtained from Wako Pure Chemicals (Kyoto, Japan). All the other chemicals and reagents were commercial products of reagent grade.

Cell Culture. OATP1B1-, OATP1B3-, and OATP2B1-expressing or vector-transfected human embryonic kidney (HEK) 293 cells were established previously (Hirano et al., 2004; Shimizu et al., 2005). HEK293 cells were grown in Dulbecco's modified Eagle's medium low glucose (Invitrogen, Carlsbad, CA) supplemented with 10% fetal bovine serum (Invitrogen), 100 U/ml penicillin, 100 μg/ml streptomycin, and 0.25 μg/ml amphotericin B at 37°C with 5% CO_2 and 95% humidity. Cells were then seeded in 12-well plates [coated with 50 mg/l poly(L-lysine) and 50 mg/l poly(L-ornithine); Sigma] at a density of 1.5×10^5 cells/well. For the transport study, the cell culture medium was replaced with culture medium supplemented with 5 mM sodium butyrate for 24 h before transport assay to induce the expression of transporters.

Transport Study Using Transporter Expression Systems. The transport study was carried out as described previously (Hirano et al., 2004). Uptake was initiated by adding Krebs-Henseleit buffer (118 mM NaCl, 23.8 mM $NaHCO_3$, 4.8 mM KCl, 1.0 mM KH_2PO_4, 1.2 mM $MgSO_4$, 12.5 mM HEPES, 5.0 mM glucose, and 1.5 mM $CaCl_2$ adjusted to pH 7.4) containing radiolabeled and unlabeled substrates after cells had been washed twice and preincubated with Krebs-Henseleit buffer at 37°C for 15 min. The uptake was terminated at designated times by adding ice-cold Krebs-Henseleit buffer after removal of the incubation buffer. Then, cells were washed twice with 1 ml of ice-cold Krebs-Henseleit buffer, solubilized in 1 N NaOH, and kept for 1 h at 37°C. Aliquots were transferred to scintillation vials after adding a half volume of 2 N HCl. The radioactivity associated with the cells and incubation buffer was measured in a liquid scintillation counter (TRI-CARB 2500TR, PerkinElmer) after adding 2 ml of scintillation fluid. The remaining 50 μl of cell lysate was used to determine the protein concentration by the method of Lowry with bovine serum albumin as a standard.

Preparation of Rat and Human Hepatocytes. Isolated rat hepatocytes were prepared from Sprague-Dawley rats weighing 200 to 300 g by the collagenase perfusion method described previously (Yamazaki et al., 1993). Isolated hepatocytes (viability >80%) were suspended in Krebs-Henseleit buffer, adjusted to 2.0×10^6 cells/ml, and stored on ice before the uptake experiment. Cryopreserved human hepatocytes (lot. OCF, MYO, and 094) were purchased from In Vitro Technologies, Inc. (Baltimore, MD). The preparation of hepatocytes was performed as described previously (Shitara et al., 2003). The cryopreserved human hepatocytes were resuspended in Krebs-Henseleit buffer to give a final cell density of 1.0×10^6 viable cells/ml for the uptake study. The number of viable cells was determined by trypan blue staining. To measure the uptake in the absence of Na^+, sodium chloride and sodium bicarbonate in Krebs-Henseleit buffer were replaced with choline chloride and choline bicarbonate.

Transport Study Using Hepatocytes. Before the uptake studies, the cell suspensions were prewarmed at 37°C for 3 min. The uptake studies were initiated by adding an equal volume of buffer (120–200 μl) containing labeled and unlabeled substrates to the cell suspension. After incubation at 37°C for 0.5, 2, or 5 min, the reaction was terminated by separating the cells from the substrate solution. For this purpose, an aliquot of 80 μl of incubation mixture was collected and placed in a centrifuge tube (450 μl) containing 50 μl of 2 N NaOH under a layer of 100 μl of oil mixture (density, 1.015, a mixture of silicone oil and mineral oil; Sigma-Aldrich), and subsequently the sample tube was centrifuged for 20 s using a standard centrifuge (17,500*g*, MX-100, TOMY). During this process, hepatocytes passed through the oil layer into the alkaline solution. After an overnight incubation in alkali to dissolve the hepatocytes and the centrifuge tube was frozen in liquid nitrogen, the centrifuge tube was cut, and each compartment was transferred to a scintillation vial. The compartment containing the dissolved cells was neutralized with 50 μl of 2 N HCl. The aliquots were mixed with scintillation mixture, and the radioactivity was measured in a liquid scintillation counter.

Estimation of Protein Unbound Concentration of Telmisartan in the Presence of Human Serum Albumin. The unbound concentration of 1 μM telmisartan in the presence of human serum albumin (HSA) (0, 0.1, 0.3, 1, 3, and 5%) was determined after a 2-h incubation at 37°C by equilibrium dialysis (DIANORM, Dainippon Pharmaceutical Ltd., Osaka, Japan).

Kinetic Analyses. Ligand uptake was expressed as the uptake volume

(microliters per milligram protein), given as the radioactivity associated with the cells (disintegrations per milligram protein) divided by its concentration in the incubation media (disintegrations per microliter). Specific uptake was obtained by subtracting the uptake into vector-transfected cells from the uptake into cDNA-transfected cells. Kinetic parameters were obtained using eq. 1:

$$v = \frac{V_{max} \times S}{K_m + S} \quad (1)$$

where v is the uptake velocity of the substrate (picomoles per minute per milligram protein), S is the substrate concentration in the medium (micromolar), K_m is the Michaelis constant (micromolar), and V_{max} is the maximum uptake rate (picomoles per minute per milligram protein). Fitting was performed by the nonlinear least-squares method using a MULTI program (Yamaoka et al., 1981). The half-inhibitory concentration (IC_{50}) of inhibitors was obtained by examining their inhibitory effects on the uptake of CCK-8, $E_2$17βG, and telmisartan based on eq. 2:

$$CL_{+I} = CL/\left(1 + \frac{I}{IC_{50}}\right) \quad (2)$$

where CL and CL_{+I} represent the uptake clearance in the absence and presence of inhibitor, respectively, and I is the concentration of inhibitor. IC_{50} values were estimated by the nonlinear least-squares method using a MULTI program (Yamaoka et al., 1981). To determine the saturable hepatic uptake clearance in rat and human hepatocytes, we first determined the hepatic uptake clearance [$CL_{(2\ min-0.5\ min)}$] (microliters per minute per 10^6 cells) by calculating the slope of the uptake volume (V_d) (microliters per 10^6 cells) between 0.5 and 2 min (eq. 3). The hepatic uptake clearance was fitted to eq. 1 by means of nonlinear least-squares regression analysis using a MULTI program (Yamaoka et al., 1981). The saturable hepatic uptake clearance (CL_{hep}) was determined by subtracting $CL_{(2\ min-0.5\ min)}$ in the presence of an excess of unlabeled substrate (excess) from that in the absence of unlabeled substrate (tracer) (eq. 4).

$$CL_{(2\ min-0.5\ min)} = \frac{V_{d,2\ min} - V_{d,0.5\ min}}{2 - 0.5} \quad (3)$$

$$CL_{hep} = CL_{(2\ min-0.5\ min),tracer} - CL_{(2\ min-0.5\ min),excess} \quad (4)$$

Estimation of the Maximum Unbound Concentration of Inhibitors at the Liver Inlet. The maximum unbound concentration at the liver inlet ($I_{in,max,u}$) was calculated from the following equation (eq. 5) as described previously (Ito et al., 1998).

$$I_{in,max,u} = \left(C_{max,blood} + \frac{k_a \cdot D \cdot F_a}{Q_h}\right) \times f_{u,blood} \quad (5)$$

where $C_{max,blood}$ and $f_{u,blood}$ are estimated by the reported values of the maximum blood concentration of drug after p.o. administration of the clinical dose (D = 160 mg) and the plasma protein unbound fraction (0.005) and blood-to-plasma concentration ratio (about 1.0) in humans (Stangier et al., 2000a,b). Q_h is the hepatic blood flow rate (96.6 l/h). To avoid the false-negative prediction, k_a is set to a theoretically maximum absorption rate constant (6/h), and F_a is set to one.

Statistical Analysis. The two-tailed Dunnett test was used to assess the significance of differences between three sets of data. Differences were considered to be statistically significant when $P < 0.05$.

Results

Uptake of Telmisartan into Isolated Rat Hepatocytes. Telmisartan was taken up into isolated rat hepatocytes in a time-dependent manner. Whereas saturation of the uptake of telmisartan by an excess of unlabeled telmisartan (40 μM) was not clearly observed in the incubation media with 0 and 0.1% HSA, it could be observed in the presence of 0.3 to 5% HSA (Fig. 2, A–F). Thus, we decided to evaluate the telmisartan uptake with more than 0.3% of HSA in the incubation media to prevent its extensive adsorption to the cells and culture materials. The protein unbound fraction of telmisartan in the incubation media with 0.3, 1, 3, and 5% HSA was 0.056, 0.018, 0.006, and 0.004, respectively. Both the uptake and the unbound fraction of telmisartan were reduced in parallel as the concentration of HSA was increased (Fig. 2G). In the presence of 1% HSA, telmisartan was taken up into isolated rat hepatocytes linearly up to 5 min (Fig. 3A). The concentration dependence of the uptake of telmisartan was studied over concentration range of 0.1 to 40 μM in the presence of 1% HSA. Eadie-Hofstee plot showed one saturable component (Fig. 3B), and the apparent K_m and V_{max} values for telmisartan uptake in the presence of 1% HSA were 21.7 ± 4.4 μM and 371 ± 58 pmol/min/10^6 cells, respectively. Depletion of Na^+ in the incubation media did not affect the uptake of telmisartan (Fig. 4A), and the uptake was inhibited by pravastatin, digoxin, and taurocholate, which are substrates and inhibitors of Oatp isoforms, with IC_{50} values of 58.6 ± 15.5, 45.3 ± 11.7, and 300 ± 99 μM, respectively. However, 1 mM TEA, a typical substrate of organic cation transporter, did not affect the uptake of telmisartan (Fig. 4B).

Uptake of Telmisartan by Transporter-Expressing HEK293 Cells. In the transport study using transporter expression systems, we reduced the HSA concentration from 1% to 0.3% in the incubation media because only a minimal transport activity of $E_2$17βG, which is used as the probe substrate for OATP1B1, was detected in OATP1B1-expressing cells in the presence of 1% HSA because of the significant decrease in its unbound concentration by binding to HSA (vector-transfected control cells, 2.32 ± 0.21 μl/2 min/mg protein; OATP1B1-expressing cells, 3.95 ± 0.21 μl/2 min/mg protein). To identify which transporters are important for the hepatic uptake of telmisartan in humans, the uptake assay was carried out using OATP1B1- and OATP1B3-expressing HEK293 cells in the presence of 0.3% HSA in the incubation media. Under these conditions, significant uptake of $E_2$17βG by OATP1B1- and OATP1B3-expressing HEK293 cells was observed (Fig. 5B). On the other hand, telmisartan was taken up by OATP1B3 but not by OATP1B1 (Fig. 5A). Because the difference in the degree of uptake between vector- and OATP1B3-transfected cells was too small to assess its saturation kinetics in the presence of 0.3% HSA, the concentration dependence of telmisartan uptake was evaluated over the concentration range of 0.05 to 10 μM in the absence of HSA at 5 min. The K_m and V_{max} values of telmisartan transport by OATP1B3 were calculated to be 0.81 ± 0.18 μM and 6.7 ± 0.91 pmol/min/mg protein, respectively (Fig. 6).

Inhibitory Effect of E-sul on OATP1B1- and OATP1B3-Mediated Uptake of Telmisartan in Transporter-Expression Systems. The inhibitory effect of E-sul on OATP1B1- and OATP1B3-mediated uptake of $E_2$17βG, CCK-8, and telmisartan was evaluated using OATP1B1- and OATP1B3-expressing HEK293 cells in the presence of 0.3% HSA. E-sul strongly inhibited OATP1B1-mediated $E_2$17βG uptake with an IC_{50} value of 0.79 ± 0.51 μM, whereas E-sul did not inhibit the OATP1B3-mediated CCK-8 uptake up to 30 μM (IC_{50} = 97.1 ± 37 μM) (Fig. 7A). In addition, the OATP1B3-mediated uptake of telmisartan was not inhibited by 30 μM E-sul (Fig. 7B).

Uptake of Telmisartan into Cryopreserved Human Hepatocytes. The uptake of 1 μM $E_2$17βG and 0.1 μM telmisartan by three different batches of cryopreserved human hepatocytes (lot. OCF, 094, and MYO) in the presence of 0.3% HSA was increased from 0.5 to 2 min [uptake of $E_2$17βG and telmisartan by cryopreserved human hepatocytes (OCF): 6.3 ± 1.0 and 56.7 ± 3.6 μl/min/10^6 cells, respectively], and their uptake was reduced in the presence of an excess of unlabeled $E_2$17βG (200 μM) and telmisartan (40 μM) to 0.6 ± 1.1 and 8.2 ± 4.7 μl/min/10^6 cells, respectively. The uptake of $E_2$17βG into human hepatocytes was inhibited by more than half at 30 μM E-sul, whereas that of telmisartan was not significantly inhibited by 30 μM E-sul (Table 1).

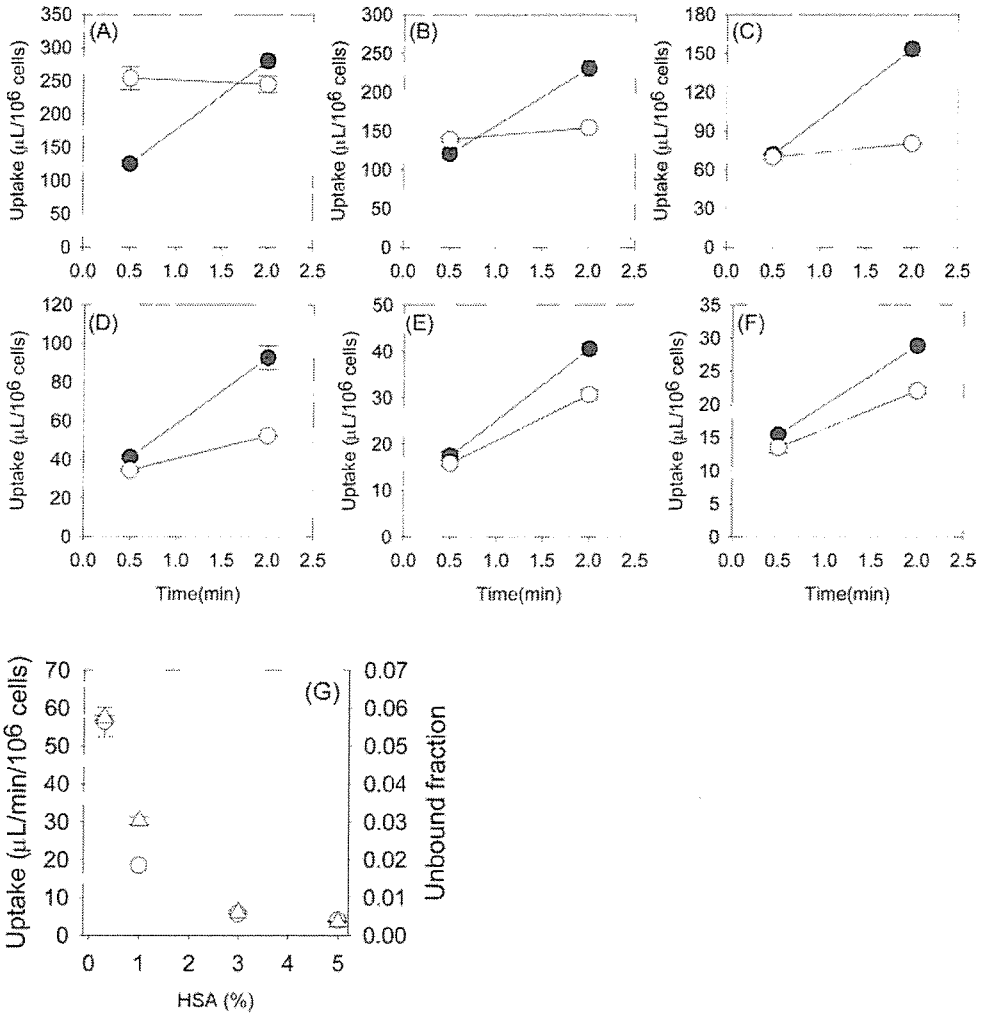

FIG. 2. Effect of various concentrations of HSA on the uptake of telmisartan in isolated rat hepatocytes and the unbound fraction of telmisartan. Uptake of telmisartan was measured by incubating cells with 0.1 μM (closed circle) and 40 μM (open circle) telmisartan, and saturable uptake of telmisartan by isolated rat hepatocytes was determined using eq. 3 and eq. 4. HSA concentrations used were 0 (A), 0.1 (B), 0.3 (C), 1 (D), 3 (E), and 5% (F). G, triangles and circles represent the uptake of telmisartan into isolated rat hepatocytes (μl/min/10^6 cells) and unbound fraction of telmisartan, respectively. Each point represents the mean ± S.E. of three separate determinations.

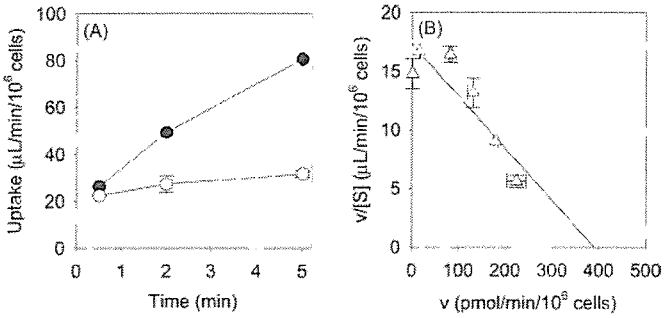

FIG. 3. Time profile (A) and Eadie-Hofstee plot (B) of the uptake of telmisartan by isolated rat hepatocytes in the presence of 1% HSA. A, substrate concentrations used were 0.1 (closed circles) and 40 μM (open circles). B, the uptake of telmisartan in isolated rat hepatocytes was measured at a concentration between 0.1 and 40 μM telmisartan. The initial uptake rate of telmisartan in isolated rat hepatocytes was determined using eq. 3. The solid line represents the fitted curve. Each point represents the mean ± S.E. of three separate determinations.

Discussion

In the present study, we have shown that telmisartan is likely to be taken up into rat and human hepatocytes by OATP family transporters because the uptake was Na^+-independent and inhibited by some OATP substrates/inhibitors. We also have suggested that OATP1B3 predominantly contributes to the hepatic uptake of telmisartan in human hepatocytes.

Because it is difficult to evaluate the transport of telmisartan in the absence of HSA because of the extensive adsorption of lipophilic telmisartan to cells and/or culture materials, we examined the effect of different concentrations of HSA (0.1–5%) in the incubation media on the uptake of telmisartan by isolated rat hepatocytes (Fig. 2, A–F). In 0.3 to 5% HSA, saturable time-dependent uptake of telmisartan was clearly observed. The uptake of telmisartan into isolated rat hepatocytes was almost proportional to the protein unbound concentration of telmisartan in the incubation media, suggesting that the uptake of telmisartan followed the "free" hypothesis, in which only unbound ligand can be recognized by transporters (Fig. 2G).

Taking the balance between the absolute uptake amount and the avoidance of extensive adsorption of telmisartan to cells and/or culture materials by HSA into consideration, we decided to use 1 and 0.3% HSA in the incubation media for the further evaluation of telmisartan uptake by rat and human hepatocytes, respectively.

Initially, we characterized the transport property of telmisartan using isolated rat hepatocytes. Telmisartan was transported into isolated rat hepatocytes in a time- and concentration-dependent manner

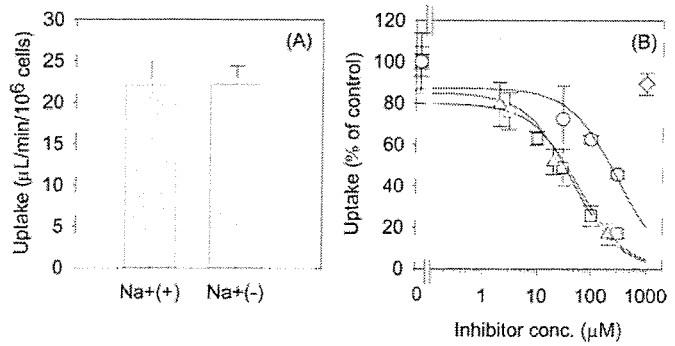

FIG. 4. Effect of Na^+ ion (A) and various compounds (B) on the uptake of telmisartan in isolated rat hepatocytes in the presence of 1% HSA. The substrate concentration used was 0.1 μM. Saturable uptake of telmisartan by isolated rat hepatocytes was determined using eq. 3 and eq. 4. B, data are shown as the percentage of the saturable uptake of telmisartan in the absence of inhibitors. Squares, triangles, circles, and diamonds represent the uptake of telmisartan in the presence of pravastatin, digoxin, taurocholate, and tetraethylammonium, respectively. Solid lines represent the fitted curves obtained by nonlinear regression analysis. Each bar and point represents the mean ± S.E. of three separate determinations.

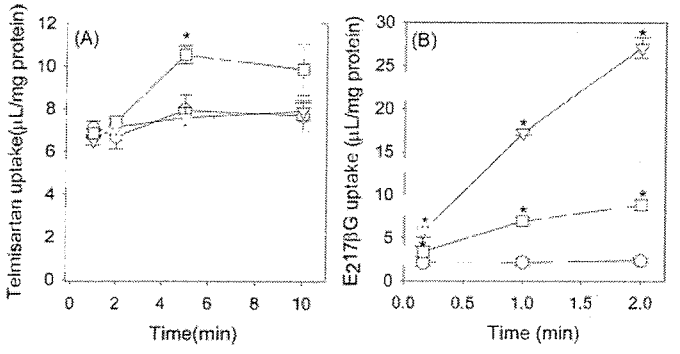

FIG. 5. Time profiles of the uptake of telmisartan (A) and $E_2$17βG (B) into transporter-expressing cells. The substrate concentrations of telmisartan and $E_2$17βG used were 0.1 μM. Squares, triangles, and circles represent the uptake by OATP1B3-, OATP1B1-, and vector-transfected cells. The uptake of telmisartan and $E_2$17βG was evaluated in the presence and absence of 0.3% HSA, respectively. *, a significant difference ($P < 0.05$) from the uptake by vector-transfected cells. Each point represents the mean ± S.E. of three separate determinations.

(Fig. 3). The K_m and V_{max} values of telmisartan uptake into isolated rat hepatocytes and the protein unbound fraction of telmisartan in the presence of 1% HSA were 21.7 μM, 371 pmol/min/10^6 cells, and 0.018, respectively. Then, the K_m value normalized by the unbound concentration in the incubation media was estimated to be 0.4 μM. To evaluate the nonsaturable uptake of telmisartan, we defined 40 μM telmisartan as an excess concentration resulting from the limited solubility of telmisartan in the incubation media. The uptake of telmisartan into isolated rat hepatocytes was Na^+-independent, indicating that telmisartan is not transported by Na^+-taurocholate cotransporting polypeptide, the uptake by which is Na^+-dependent (Fig. 4A). Furthermore, the uptake of telmisartan was inhibited by digoxin, pravastatin, and taurocholate with the IC_{50} value of 45.3, 58.6, and 300 μM, respectively. In contrast, a high concentration of TEA (1 mM) did not inhibit telmisartan uptake (Fig. 4B). Taurocholate, pravastatin, and digoxin are the substrates and inhibitors of Oatp1a1, 1a4, and 1b2 in rats (Noe et al., 1997; Kouzuki et al., 1999; Tokui et al., 1999; Cattori et al., 2000; Sasaki et al., 2004). It is reported that 100 μM digoxin completely inhibited the Oatp1a4 activity, but at most inhibited Oatp1a1-mediated uptake of digoxin by 70% (Shitara et al., 2002). Based on these results, it appears that telmisartan is taken up

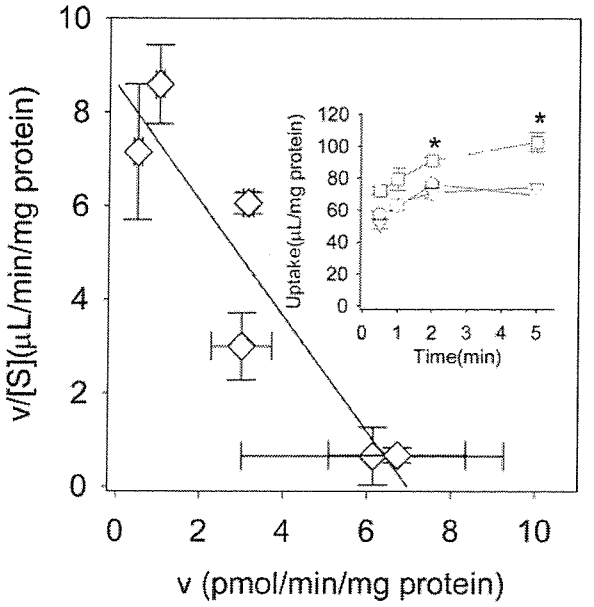

FIG. 6. Time profile and Eadie-Hofstee plot of the uptake of telmisartan into transporter-expressing cells in the absence of HSA. Inset, the substrate concentration used was 0.1 μM. Squares, triangles, and circles represent the uptake by OATP1B3-, OATP1B1-, and vector-transfected cells. The uptake of telmisartan by transporter-expressing cells was measured at a concentration between 0.05 and 10 μM telmisartan in the absence of HSA. The OATP1B3-mediated telmisartan transport was obtained by subtracting the uptake in vector-transfected cells from that in OATP1B3-expressing cells for 5 min. *, a significant difference ($P < 0.05$) from the uptake by vector-transfected cells. Each point represents the mean ± S.E. of three separate determinations.

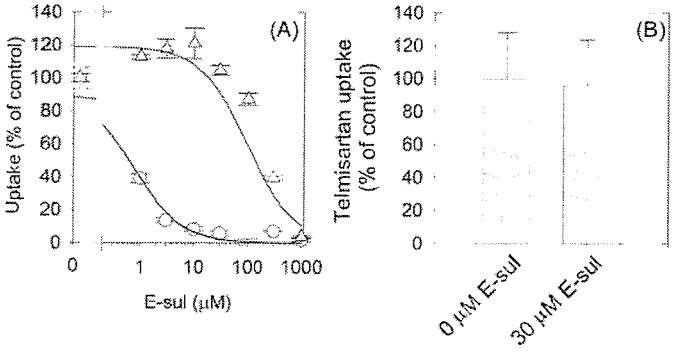

FIG. 7. Inhibitory effect of E-sul on OATP1B1-mediated $E_2$17βG uptake (A, circle), OATP1B3-mediated CCK-8 uptake (A, triangle), and OATP1B3-mediated telmisartan uptake (B) in the presence of 0.3% HSA. The substrate concentration used was 0.1 μM for all the compounds. The OATP1B1- and OATP1B3-mediated transport was obtained by subtracting the uptake in vector-transfected cells from that in OATP1B1- or OATP1B3-expressing cells for 2 min for $E_2$17βG or 5 min for CCK-8 and telmisartan. Data are shown as the percentage of the OATP1B1- and OATP1B3-mediated substrate uptake in the absence of E-sul. The solid lines in A represent the fitted curves obtained by nonlinear regression analysis. Each bar and point represents the mean ± S.E. ($n = 3$).

into rat hepatocytes by Oatp isoforms, and at least Oatp1a4 is involved in the uptake of telmisartan.

Next, to examine which human OATP transporters are involved in the uptake of telmisartan into human hepatocytes, we evaluated the transport properties of telmisartan using HEK293 cells expressing individual OATP and cryopreserved human hepatocytes. In this transport study, we reduced the HSA concentration from 1% to 0.3% in the incubation media because no significant uptake of $E_2$17βG, which is used as a probe substrate for OATP1B1, was detected in OATP1B1-expressing cells in the presence of 1% HSA. Telmisartan could be

TABLE 1

Effect of E-sul on the uptake of telmisartan and $E_2 17\beta$ G by cryopreserved human hepatocytes in the presence of 0.3% HSA

The substrate concentration used was 0.1 and 1 μM for telmisartan and $E_2 17\beta$ G. Saturable uptake of telmisartan and $E_2 17\beta$ G into cryopreserved human hepatocytes was determined after the subtraction of nonsaturable uptake (evaluated as the uptake clearance of the respective compounds in the presence of 40 μM telmisartan and 200 μM $E_2 17\beta$ G). In parentheses is the percentage of the saturable uptake of telmisartan and $E_2 17\beta$ G in the absence of inhibitor.

E-sul	HH-OCF		HH-094		HH-MYO	
	Telmisartan	$E_2 17\beta$G	Telmisartan	$E_2 17\beta$G	Telmisartan	$E_2 17\beta$G
	μl/min/10^6 cells		*μl/min/10^6 cells*		*μl/min/10^6 cells*	
0 μM	48.5 ± 3.6	5.66 ± 1.1	42.0 ± 1.7	1.85 ± 0.72	16.8 ± 5.3	2.01 ± 0.62
30 μM	63.9 ± 11 (131%)	1.50 ± 0.75 (26.6%)	42.2 ± 0.41 (100%)	1.03 ± 0.76 (55.8%)	18.1 ± 3.7 (108%)	0.38 ± 0.45 (19.0%)

taken up by OATP1B3 but not by OATP1B1 (Fig. 5A). Because the transporter-mediated uptake of telmisartan in the presence of HSA was not high enough to evaluate the saturation kinetics, we investigated the saturable uptake of telmisartan in the absence of HSA. The K_m and V_{max} values of telmisartan uptake by OATP1B3 in the absence of HSA were 0.81 μM and 6.7 pmol/min/mg protein, respectively (Fig. 6). This K_m value was almost comparable with that in isolated rat hepatocytes normalized by the unbound concentration of telmisartan in the incubation media. Telmisartan was taken up into cryopreserved human hepatocytes in a saturable manner. Considering that telmisartan was taken up by OATP1B3, but not by OATP1B1, the uptake of telmisartan seems to be mediated by OATP1B3. To confirm the minor contribution of OATP1B1 to the hepatic uptake of telmisartan, we planned to perform an inhibition study using OATP1B1- and OATP1B3-selective inhibitor. From our analyses, E-sul inhibited OATP1B1-mediated $E_2 17\beta$G uptake with an IC_{50} value of 0.8 μM, whereas E-sul did not inhibit OATP1B3-mediated CCK-8 uptake up to 30 μM (Fig. 7A). These results confirmed that 30 μM E-sul can selectively inhibit the OATP1B1-mediated uptake. On the other hand, CCK-8 inhibited both OATP1B1- and OATP1B3-mediated $E_2 17\beta$G uptake with IC_{50} value of 6.79 ± 0.59 and 14.6 ± 2.2 μM, respectively, indicating that CCK-8 cannot be used as a selective inhibitor for OATP1B3 as reported previously (Nozawa et al., 2003). The uptake of telmisartan into OATP1B3-expressing cells and cryopreserved human hepatocytes was not inhibited by 30 μM E-sul (Fig. 7B; Table 1). On the contrary, 30 μM E-sul inhibited more than half of $E_2 17\beta$G uptake in all the batches of cryopreserved human hepatocytes (Table 1). Hirano et al. (2004) have reported that the uptake of $E_2 17\beta$G in human hepatocytes is mediated mainly by OATP1B1. These results suggest that telmisartan is transported into cryopreserved human hepatocytes by OATP1B3 rather than OATP1B1.

In a previous study, the ratio of the relative expression level of OATP1B1 and OATP1B3 in cryopreserved human hepatocytes to that in expression systems, determined by Western blot analysis, was 1.79 and 0.96, respectively (Hirano et al., 2004). In human liver, OATP2B1 is also expressed on the basolateral membrane (Kullak-Ublick et al., 2001). We checked that telmisartan was significantly taken up into OATP1B3- and OATP2B1-expressing HEK293 cells (2.6 ± 0.4 and 1.7 ± 0.9 μl/5 min/mg protein, respectively). The ratio of the protein expression level of OATP2B1 in human hepatocytes to that in our expression systems was less than 0.2 (Hirano et al., 2006). Therefore, it is suggested that the contribution of OATP2B1 to the hepatic uptake of telmisartan into human hepatocytes is at most one-fifth that of OATP1B3.

In general, it is accepted that OATP1B1 is responsible for the hepatic uptake of several compounds. Hirano et al. (2004) have shown that pitavastatin and $E_2 17\beta$G are taken up mainly via OATP1B1. However, a recent report suggested that fexofenadine, an H_1-receptor antagonist, is transported by OATP1B3 rather than OATP1B1 (Shimizu et al., 2005). Moreover, in the case of valsartan, which is in the same therapeutic class as telmisartan, the contribution of OATP1B1 and OATP1B3 to its hepatic uptake is estimated to be almost similar (Yamashiro et al., 2006). Therefore, the relative contribution of OATP1B1 and OATP1B3 to the hepatic uptake of organic anions depends on the substrate properties and chemical structures, and we cannot a priori decide which transporters are responsible for hepatic uptake without using dedicated experiments for estimating the contribution of each proposed transporter.

The C_{max} value of telmisartan increases disproportionately with the dose (10–160 mg). In clinical situations, 160/25 mg/day telmisartan/hydrochlorothiazide combination therapy is approved for the treatment of hypertension in the United States. The C_{max} values of telmisartan after single and multiple 160-mg doses were 3.0 and 5.6 μM, respectively (Stangier et al., 2000b). Considering that 99.5% of the telmisartan in blood is bound to plasma proteins (Stangier et al., 2000b), the unbound concentration of telmisartan is estimated to be 0.015 and 0.028 μM. These values are more than 20 times lower than the K_m value of telmisartan uptake by OATP1B3 obtained in this study. In addition, to avoid the false-negative prediction of the contribution of OATP1B3 to its nonlinear pharmacokinetics, we calculated the maximum unbound concentration of telmisartan at the inlet to the liver ($I_{in,\ max,\ u}$) to be 0.12 μM after multiple 160-mg doses using an established method (Ito et al., 1998). However, the K_m value of telmisartan uptake by OATP1B3 is still more than 5 times higher than the $I_{in,\ max,\ u}$ of telmisartan. If the conventional assumption applies, in which only the unbound drug can interact with OATP1B3, the saturation of OATP1B3-mediated telmisartan uptake seems to have a minor effect on the nonlinear increase of C_{max} and AUC over the clinical dose range. Furthermore, a large interindividual variability in the plasma profile of telmisartan has been observed in clinical situations (Stangier et al., 2000a,c). Letschert et al. (2004) have reported two naturally occurring mutations in the *SLCO1B3* gene that cause a substrate-dependent functional change in OATP1B3. The genetic polymorphisms in OATP1B3 may be one of the reasons for the interindividual variability of the pharmacokinetics of telmisartan. In addition, the glucuronidation process of telmisartan and hepatobiliary transport of telmisartan glucuronide may also affect its interindividual variability, and further quantitative analyses in each process will be needed.

In conclusion, we have shown that telmisartan is taken up into human hepatocytes by OATP1B3 rather than by OATP1B1. In addition, these findings support and further extend the important role of OATP1B3 in overall hepatic elimination of some drugs.

References

Abe T, Kakyo M, Tokui T, Nakagomi R, Nishio T, Nakai D, Nomura H, Unno M, Suzuki M, Naitoh T, et al. (1999) Identification of a novel gene family encoding human liver-specific organic anion transporter LST-1. *J Biol Chem* **274**:17159–17163.

Cattori V, Hagenbuch B, Hagenbuch N, Stieger B, Ha R, Winterhalter KE, and Meier PJ (2000)

Identification of organic anion transporting polypeptide 4 (Oatp4) as a major full-length isoform of the liver-specific transporter-1 (rlst-1) in rat liver. *FEBS Lett* **474**:242–245.
Faber KN, Muller M, and Jansen PL (2003) Drug transport proteins in the liver. *Adv Drug Deliv Rev* **55**:107–124.
Hagenbuch B and Meier PJ (2003) The superfamily of organic anion transporting polypeptides. *Biochim Biophys Acta* **1609**:1–18.
Hedner T (1999) Management of hypertension: the advent of a new angiotensin II receptor antagonist. *J Hypertens Suppl* **17**:S21–S25.
Hirano M, Maeda K, Shitara Y, and Sugiyama Y (2004) Contribution of OATP2 (OATP1B1) and OATP8 (OATP1B3) to the hepatic uptake of pitavastatin in humans. *J Pharmacol Exp Ther* **311**:139–146.
Hirano N, Maeda K, Shitara Y, and Sugiyama Y (2006) Drug-drug interaction between pitavastatin and various drugs via OATP1B1. *Drug Metab Dispos* **34**:1229–1236.
Hsiang B, Zhu Y, Wang Z, Wu Y, Sasseville V, Yang WP, and Kirchgessner TG (1999) A novel human hepatic organic anion transporting polypeptide (OATP2). Identification of a liver-specific human organic anion transporting polypeptide and identification of rat and human hydroxymethylglutaryl-CoA reductase inhibitor transporters. *J Biol Chem* **274**:37161–37168.
Ismair MG, Stieger B, Cattori V, Hagenbuch B, Fried M, Meier PJ, and Kullak-Ublick GA (2001) Hepatic uptake of cholecystokinin octapeptide by organic anion-transporting polypeptides OATP4 and OATP8 of rat and human liver. *Gastroenterology* **121**:1185–1190.
Ito K, Iwatsubo T, Kanamitsu S, Ueda K, Suzuki H, and Sugiyama Y (1998) Prediction of pharmacokinetic alterations caused by drug-drug interactions: metabolic interaction in the liver. *Pharmacol Rev* **50**:387–412.
Kok LD, Siu SS, Fung KP, Tsui SK, Lee CY, and Waye MM (2000) Assignment of liver-specific organic anion transporter (SLC22A7) to human chromosome 6 bands p21.2→p21.1 using radiation hybrids. *Cytogenet Cell Genet* **88**:76–77.
Konig J, Cui Y, Nies AT, and Keppler D (2000a) A novel human organic anion transporting polypeptide localized to the basolateral hepatocyte membrane. *Am J Physiol* **278**:G156–G164.
Konig J, Cui Y, Nies AT, and Keppler D (2000b) Localization and genomic organization of a new hepatocellular organic anion transporting polypeptide. *J Biol Chem* **275**:23161–23168.
Kouzuki H, Suzuki H, Ito K, Ohashi R, and Sugiyama Y (1999) Contribution of organic anion transporting polypeptide to uptake of its possible substrates into rat hepatocytes. *J Pharmacol Exp Ther* **288**:627–634.
Kullak-Ublick GA, Ismair MG, Stieger B, Landmann L, Huber R, Pizzagalli F, Fattinger K, Meier PJ, and Hagenbuch B (2001) Organic anion-transporting polypeptide B (OATP-B) and its functional comparison with three other OATPs of human liver. *Gastroenterology* **120**:525–533.
Letschert K. Keppler D, and Konig J (2004) Mutations in the SLCO1B3 gene affecting the substrate specificity of the hepatocellular uptake transporter OATP1B3 (OATP8) *Pharmacogenetics* **14**:441–452.
Noe B, Hagenbuch B, Stieger B, and Meier PJ (1997) Isolation of a multispecific organic anion and cardiac glycoside transporter from rat brain. *Proc Natl Acad Sci USA* **94**:10346–10350.
Nozawa T, Tamai I, Sai Y, Nezu J, and Tsuji A (2003) Contribution of organic anion transporting polypeptide OATP-C to hepatic elimination of the opioid pentapeptide analogue [D-Ala2, D-Leu5]-enkephalin. *J Pharm Pharmacol* **55**:1013–1020.
Oliverio MI and Coffman TM (1997) Angiotensin-II-receptors: new targets for antihypertensive therapy. *Clin Cardiol* **20**:3–6.
Ries UJ, Mihm G, Narr B, Hasselbach KM, Wittneben H, Entzeroth M, van Meel JC, Wienen W, and Hauel NH (1993) 6-Substituted benzimidazoles as new nonpeptide angiotensin II receptor antagonists: synthesis, biological activity and structure-activity relationships. *J Med Chem* **36**:4040–4051.
Sasaki M, Suzuki H, Aoki J, Ito K, Meier PJ, and Sugiyama Y (2004) Prediction of in vivo biliary clearance from the in vitro transcellular transport of organic anions across a double-transfected Madin-Darby canine kidney II monolayer expressing both rat organic anion transporting polypeptide 4 and multidrug resistance associated protein 2. *Mol Pharmacol* **66**:450–459.
Shimizu M, Fuse K, Okudaira K, Nishigaki R, Maeda K, Kusuhara H, and Sugiyama Y (2005) Contribution of OATP (organic anion-transporting polypeptide) family transporters to the hepatic uptake of fexofenadine in humans. *Drug Metab Dispos* **33**:1477–1481.
Shitara Y, Li AP, Kato Y, Lu C, Ito K, Itoh T, and Sugiyama Y (2003) Function of uptake transporters for taurocholate and estradiol 17beta-D-glucuronide in cryopreserved human hepatocytes. *Drug Metab Pharmacokinet* **18**:33–41.
Shitara Y, Sugiyama D, Kusuhara H, Kato Y, Abe T, Meier PJ, Itoh T, and Sugiyama Y (2002) Comparative inhibitory effects of different compounds on rat oatp1 (slc21a1)- and Oatp2 (Slc21a5)-mediated transport. *Pharm Res (NY)* **19**:147–153.
Stangier J, Schmid J, Turck D, Switek H, Verhagen A, Peeters PA, van Marle SP, Tamminga WJ, Sollie FA, and Jonkman JH (2000a) Absorption, metabolism and excretion of intravenously and orally administered [^{14}C]telmisartan in healthy volunteers. *J Clin Pharmacol* **40**:1312–1322.
Stangier J, Su CA, and Roth W (2000b) Pharmacokinetics of orally and intravenously administered telmisartan in healthy young and elderly volunteers and in hypertensive patients. *J Int Med Res* **28**:149–167.
Stangier J, Su CA, Schondorfer G, and Roth W (2000c) Pharmacokinetics and safety of intravenous and oral telmisartan 20 mg and 120 mg in subjects with hepatic impairment compared with healthy volunteers. *J Clin Pharmacol* **40**:1355–1364.
Tamai I, Nezu J, Uchino H, Sai Y, Oku A, Shimane M, and Tsuji A (2000) Molecular identification and characterization of novel members of the human organic anion transporter (OATP) family. *Biochem Biophys Res Commun* **273**:251–260.
Tokui T, Nakai D, Nakagomi R, Yawo H, Abe T, and Sugiyama Y (1999) Pravastatin, an HMG-CoA reductase inhibitor, is transported by rat organic anion transporting polypeptide, oatp2. *Pharm Res (NY)* **16**:904–908.
Vavricka SR, Van Montfoort J, Ha HR, Meier PJ, and Fattinger K (2002) Interactions of rifamycin SV and rifampicin with organic anion uptake systems of human liver. *Hepatology* **36**:164–172.
Wienen W, Entzeroth M, van Meel JCA, Stangier J, Busch U, Ebner T, Schmid J, Lehmann H, Matzek K, Kempthorne-Rawson J, et al. (2000) A review on telmisartan: a novel long-acting angiotensin II-receptor antagonist. *Cardiovasc Drug Rev* **18**:127–156.
Yamaoka K, Tanigawara Y, Nakagawa T, and Uno T (1981) A pharmacokinetic analysis program (multi) for microcomputer. *J Pharmacobio-Dyn* **4**:879–885.
Yamashiro W, Maeda K, Hirouchi M, Adachi Y, Hu Z, and Sugiyama Y (2006) Involvement of transporters in the hepatic uptake and biliary excretion of valsartan, a selective antagonist of the angiotensin II AT1-receptor, in humans. *Drug Metab Dispos* **34**:1247–1254.
Yamazaki M, Suzuki H, Hanano M, Tokui T, Komai T, and Sugiyama Y (1993) Na(+)-independent multispecific anion transporter mediates active transport of pravastatin into rat liver. *Am J Physiol* **264**:G36–G44.

Address correspondence to: Dr. Yuichi Sugiyama, Department of Molecular Pharmacokinetics, Graduate School of Pharmaceutical Sciences, The University of Tokyo, 7-3-1 Hongo, Bunkyo-ku, Tokyo 113-0033, Japan. E-mail: sugiyama@mol.f.u-tokyo.ac.jp

0090-9556/06/3409-1575–1581$20.00
DRUG METABOLISM AND DISPOSITION
Vol. 34, No. 9
8748/3132909
Printed in U.S.A.

DMD 34:1575–1581, 2006

Inhibition of Bile Acid Transport across Na^+/Taurocholate Cotransporting Polypeptide (SLC10A1) and Bile Salt Export Pump (ABCB 11)-Coexpressing LLC-PK1 Cells by Cholestasis-Inducing Drugs

Sachiko Mita, Hiroshi Suzuki, Hidetaka Akita,[1] Hisamitsu Hayashi, Reiko Onuki, Alan F. Hofmann, and Yuichi Sugiyama

Graduate School of Pharmaceutical Sciences, The University of Tokyo, Tokyo, Japan (S.M., H.S., H.A., H.H., R.O., Y.S.); and Department of Medicine, University of California, La Jolla, California (A.H.)

Received December 2, 2005; accepted June 5, 2006

ABSTRACT:

Vectorial transport of bile acids across hepatocytes is a major driving force for bile flow, and bile acid retention in the liver causes hepatotoxicity. The basolateral and apical transporters for bile acids are thought to be targets of drugs that induce cholestasis. Previously, we constructed polarized LLC-PK1 cells that express both a major bile acid uptake transporter human Na^+/taurocholate cotransporting polypeptide (SLC10A1) (NTCP) and the bile acid efflux transporter human bile salt export pump (ABCB 11) (BSEP) and showed that monolayers of such cells can be used to characterize vectorial transcellular transport of bile acids. In the present study, we investigated whether cholestasis-inducing drugs could inhibit bile acid transport in such cells. Because fluorescent substrates allow the development of a high-throughput screening method, we examined the transport by NTCP and BSEP of fluorescent bile acids as well as taurocholate. The aminofluorescein-tagged bile acids, chenodeoxycholylglycylamidofluorescein and cholylglycylamidofluorescein, were substrates of both NTCP and BSEP, and their basal-to-apical transport rates across coexpressing cell monolayers were 4.3 to 4.5 times those of the vector control, although smaller than for taurocholate. The well known cholestatic drugs, rifampicin, rifamycin SV, glibenclamide, and cyclosporin A, reduced the basal-to-apical transport and the apical efflux clearance of taurocholate across NTCP- and BSEP-coexpressing cell monolayers. Further analysis indicated that the drugs inhibited both NTCP and BSEP. Our study suggests that such coexpressing cells can provide a useful system for the identification of inhibitors of these two transport systems, including potential drug candidates.

Hepatotoxic adverse effects, often indicated by cholestasis, are a concern for every drug, and severe hepatotoxicity may cause a drug to be withdrawn from the market. Biliary excretion of bile acids is one of the principal driving forces for bile formation by generating an osmotic driving force favoring influx of water and electrolytes through the paracellular space (Wheeler et al., 1968; Wheeler, 1972). The transcellular transport is mediated by transporter proteins located on the sinusoidal (basolateral) and canalicular (apical) membranes of hepatocytes (Meier and Stieger, 2002; Trauner and Boyer, 2003). The basolateral Na^+/taurocholate cotransporting polypeptide (NTCP/SLC10A1) transports bile acids from the space of Disse into hepatocytes (Hagenbuch et al., 1991; Boyer et al., 1994). Human NTCP accepts most physiological bile acids and some organic anions, such as estrone-3-sulfate and bromosulfophthalein (Meier et al., 1997). Sodium-independent uptake of bile acids is carried out by members of the organic anion-transporting polypeptide family, such as rat Oatp1a1 and human OATP1B1. Although there are several carrier proteins capable of transporting bile acids, much evidence suggests, at least in the rodent, that NTCP-mediated transport accounts for a large part of the total bile acid uptake (Wolkoff and Cohen, 2003). At the canalicular membrane, the efflux of bile acids by the bile salt export pump (BSEP/ABCB11) mediates concentrative excretion (Boyer et al., 1994; Gerloff et al., 1998; Noe et al., 2002). Mutations of BSEP in humans causes progressive familial intrahepatic cholestasis type II, a fatal condition (Strautnieks et al., 1998).

One mechanism for cholestasis is thought to be inhibition of hepatocyte transport systems for bile acids and other organic anions by

This study was supported by a Grant-in-Aid for Scientific Research on Priority Areas Epithelial Vectorial Transport 12144201, a Grant-in-Aid for Center of Excellence (COE) from The Ministry of Education, Culture, Sports, Science and Technology of Japan, and National Institutes of Health Grant DK 64891 at University of California, San Diego.

[1] Current affiliation: Graduate School of Pharmaceutical Sciences, Hokkaido University, Sapporo, Japan.

Article, publication date, and citation information can be found at http://dmd.aspetjournals.org.

doi:10.1124/dmd.105.008748.

ABBREVIATIONS: NTCP, Na^+/taurocholate cotransporting polypeptide (SLC10A1); BSEP, bile salt export pump (ABCB 11); CGamF, cholylglycylamidofluorescein; CamF, cholylamidofluorescein; CDCGamF, chenodeoxycholylglycylamidofluorescein; NBD, 7-nitrobenz-2-oxa-1,3-diazol-4-yl; UDC-L-NBD, ursodeoxycholyl-(N-ε-NBD)-lysine; 7β-NBD-NCT, 7β-NBD-cholyltaurine; PS, permeability-surface area product; LLC-NTCP/BSEP, NTCP- and BSEP-coexpressing LLC-PK1 cells; LLC-NTCP, NTCP-expressing LLC-PK1 cells.

drugs. The inhibitory effects of such drugs on the uptake and efflux of bile acids have been studied using isolated and primary cultured hepatocyte or canalicular membrane vesicles (Kukongviriyapan and Stacey, 1991), as well as the isolated perfused liver (Bolder et al., 1999). Recently, NTCP and BSEP, which generate bile salt-dependent bile flow, have been shown to be possible target molecules for cholestatic drugs (Kim et al., 1999; Stieger et al., 2000; Akita et al., 2001; Bohan and Boyer, 2002).

Previously, we constructed NTCP- and BSEP-coexpressing LLC-PK1 cells as an in vitro model of the vectorial transcellular transport of bile acids in hepatocytes (Mita et al., 2006). This approach is useful for the screening of choleretic bile acids, which are good substrates of these transporters. A second use of this system is to identify inhibitors of these transporters which might have cholestatic effects in vivo. The method should also be useful for defining structure-transport activity relationships of bile acids. In the present study, we assessed the inhibitory effects of cholestasis-inducing drugs on transport across coexpressing cells with the aim of developing a screening system for cholestatic compounds. We compared the transport of fluorescent bile acid derivatives with that of taurocholate in the hope that such fluorescent compounds would be efficiently transported and thereby permit the development of a high-throughput screening method for detecting the inhibitory effects of drug candidates.

Materials and Methods

Chemicals. [^{3}H]Taurocholic acid (2 Ci/mmol) was purchased from PerkinElmer Life Sciences (Boston, MA). Unlabeled taurocholic acid was obtained from Sigma Chemical Co. (St. Louis, MO). Unlabeled cholic acid was purchased from Wako Pure Chemicals Industries, Ltd. (Osaka, Japan). Unlabeled ursodeoxycholic acid, tauroursodeoxycholic acid, and glycoursodeoxycholic acid were kindly provided by Mitsubishi Pharma (Osaka, Japan). Fluorescent bile acids [cholylglycylamidofluorescein (CGamF), cholylamidofluorescein (CamF), chenodeoxycholylglycylamidofluorescein (CDCGamF), ursodeoxycholyl-(Nε-NBD)-lysine (UDC-L-NBD), and 7β-NBD-cholyltaurine (7β-NBD-NCT)] were synthesized in the laboratory of Alan F. Hofmann as described previously (Sorscher et al., 1992; Holzinger et al., 1998). The following compounds were obtained from Sigma-Aldrich (St. Louis, MO): cyclosporin A, rifampicin, rifamycin SV, and glibenclamide. All other chemicals used were commercially available and of reagent grade.

Cell Culture and Transfection. Human NTCP- and human BSEP-expressing LLC-PK1 cells were established and maintained as described previously (Mita et al., 2006). Briefly, parental LLC-PK1 cells were grown in M199 media (Invitrogen, Carlsbad, CA) supplemented with 10% fetal bovine serum and 1% antibiotic-antimycotic (Invitrogen; 100 U/ml penicillin, 100 μg/ml streptomycin, 0.25 μg/ml amphotericin B) at 37°C under 5% CO_2. Full-length human NTCP cDNA was subcloned into pcDNA3.1 (Invitrogen) and transfected into LLC-PK1 cells with FuGENE 6 (Roche Diagnostics Corporation, Indianapolis, IN) according to the manufacturer's instructions. Transfectants expressing NTCP were selected with G418 (800 μg/ml) and the clone with the highest NTCP activity was screened by the uptake activity for taurocholate. The BD Adeno-X Adenoviral Expression System (BD Biosciences, Palo Alto, CA) was used to establish the recombinant adenovirus encoding human BSEP (Hayashi et al., 2005). Forty-eight hours before each experiment, LLC-PK1 cells were infected by the recombinant adenoviruses or control viruses containing green fluorescent protein at a multiplicity of infection of 100.

Transport Studies. NTCP- or mock-transfected LLC-PK1 cells were seeded on Transwell membrane inserts (pore size of 3 μm; Falcon, Bedford, MA) in 12-well plates at a density of 1.4×10^5 cells per insert for transcellular transport studies, cultured at confluence for 2 days, and infected by recombinant adenovirus containing cDNAs for BSEP or GFP (100 multiplicity of infection). For uptake studies, NTCP- or mock-transfected LLC-PK1 cells were seeded on 12-well plates and cultured without viral infection. Cells were harvested 48 h after infection, and expression of NTCP was induced by 10 mM sodium butyrate for 24 h (Cui et al., 1999). To evaluate the integrity of the monolayer, transepithelial electrical resistance was measured using a Millicell-ERS (Millipore Corp., Bedford, MA). The monolayers' transepithelial electrical resistances before the experiments were 200 to 300 Ω cm^2. Then, cells were washed with transport buffer (118 mM NaCl, 23.8 mM $NaHCO_3$, 4.83 mM KCl, 0.96 mM KH_2PO_4, 1.20 mM $MgSO_4$, 12.5 mM HEPES, 5 mM glucose, and 1.53 mM $CaCl_2$ adjusted to pH 7.4). Subsequently, ^{3}H-labeled taurocholate or fluorescent bile acids were added to the transport buffer in the basal compartment (950 μl) for transcellular transport studies or 12-well plates for uptake studies. After the times indicated, the amount of substrates in the opposite apical compartment was measured by the radioactivity for taurocholate, or by the absorbance at 490 nm for fluorescent bile acids using a Microplate Spectrophotometer (Molecular Devices, Sunnyvale, CA). Potential inhibitors were added to both apical and basal compartments 30 min before the transport study. The accumulated radioactivity in the cell was determined at the end of the experiments by lysing the cells with 500 μl of 0.2 N NaOH and measuring the radioactivity in the cell lysates. Aliquots (50 μl) of cell lysate were used to determine protein concentrations by the method of Lowry et al. (1951) with bovine serum albumin as a standard. The apparent intracellular concentration of taurocholate (C_{cell}) was determined by assuming that the cellular volume per milligram of cellular protein was 4 μl.

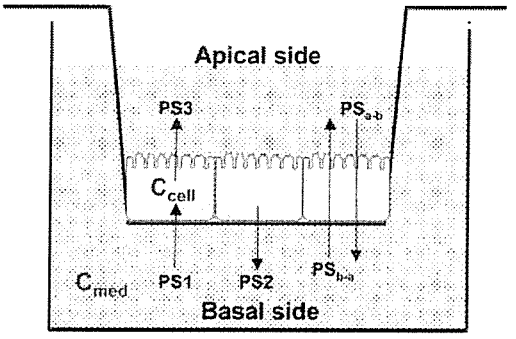

FIG. 1. Schematic diagram illustrating transcellular transport across LLC-PK1 monolayers. PS_{b-a} (μl/min/mg protein) is the PS product for the basal-to-apical clearance defined for the ligand concentration in the medium [C_{med} (pmol/μl)]. PS1 (μl/min/mg protein) is the PS product for the influx of ligand across the basal membrane, which is defined for C_{med}. PS3 (μl/min/mg protein) is the PS product for the efflux of ligand across the apical membrane, which is defined for the ligand concentration in the cells [C_{cell} (pmol/μl)]. PS2 (μl/min/mg protein) is the PS product for the efflux of ligand across the basal membrane from the cell to the basal compartment, which is defined for C_{cell}.

Data Analysis. The kinetic parameters were defined as follows: PS_{b-a} (μl/min/mg protein) is the permeability-surface area product (PS) for the basal-to-apical clearance defined for the ligand concentration in the medium [C_{med} (pmol/μl)] (Fig. 1). PS1 (μl/min/mg protein) is the PS product for the influx of ligand across the basal membrane, which is defined for C_{med}; PS3 (μl/min/mg protein) is the PS product for the efflux of ligand across the apical membrane, which is defined for the ligand concentration in the cells [C_{cell} (pmol/μl)]; and PS2 (μl/min/mg protein) is the PS product for the efflux of ligand across the basal membrane from the cell to the basal compartment, which is defined for C_{cell}. PS_{b-a} is given as a hybrid parameter consisting of PS1, PS2, and PS3 (Mita et al., 2005): $PS_{b-a} = PS1 \cdot PS3/(PS2 + PS3)$.

In this study, PS_{b-a} and PS3 of taurocholate were calculated as follows: $PS_{b-a} = V_{apical}/C_{med}$ and $PS3 = V_{apical}/C_{cell}$, where V_{apical} (pmol/min/mg protein) is the increasing velocity of taurocholate in the apical compartment. V_{apical} was determined by analyzing the transcellular transport for 1 h. Since the amount of taurocholate transported increased linearly as a function of time over the 2-h period and the intracellular concentration was constant during the incubation periods (Mita et al., 2006), we hypothesized that the initial transport velocity could be determined from the slope over the period 0 to 1 h.

Results

Transcellular Transport of Fluorescent Bile Acids. To identify a good substrate of NTCP and BSEP for the functional probe in the inhibition study, the basal-to-apical transport clearance (PS_{b-a}) of taurocholate and fluorescent bile acids across NTCP- and BSEP-coexpressing LLC-PK1 cells (LLC-NTCP/BSEP) was compared

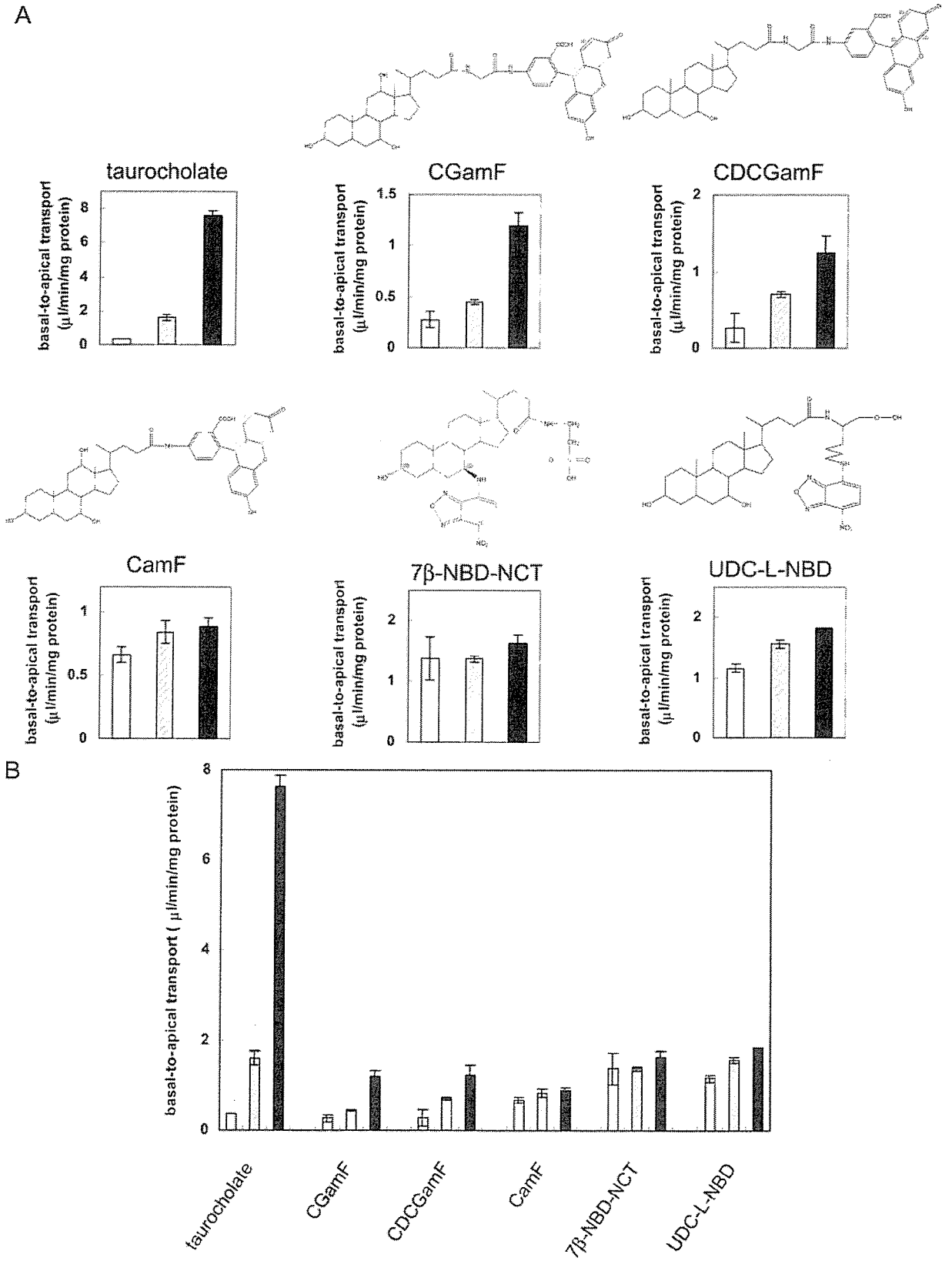

FIG. 2. Transcellular transport of labeled and fluorescent bile acids across NTCP- and BSEP-coexpressing LLC-PK1 cells. [^{3}H]Taurocholate (1 μM), CGamF, CamF, CDCGamF, UDC-L-NBD, and 7β-NBD-NCT (10 μM) across the LLC-PK1 cell monolayers were determined. Open, hatched, and closed bars represent the basal-to-apical transcellular transport across the control (LLC), LLC-NTCP, and LLC-NTCP/BSEP monolayers, respectively. Vertical bars represent the S.E. of three determinations. At the bottom is a graph in which the transcellular transport data are expressed on the same scale.

TABLE 1

Transcellular transport of labeled and fluorescent bile acids across NTCP and BSEP coexpressing LLC-PK1 cells

Data are expressed as mean ± S.E.

	Basal-to-Apical Transport		Ratio (NTCP/BSEP/Control)
	LLC-PK1 (control)	LLC-NTCP/ BSEP	
	μl/min/mg protein		
Taurocholate	0.36 ± 0.00	7.62 ± 0.26	20.94
CGamF	0.28 ± 0.08	1.19 ± 0.13	4.32
CDCGamF	0.27 ± 0.18	1.24 ± 0.22	4.61
CamF	0.66 ± 0.06	0.89 ± 0.07	1.33
7β-NBD-NCT	1.38 ± 0.35	1.63 ± 0.13	1.18
UDC-L-NBD	1.16 ± 0.07	1.83 ± 0.00	1.58

(Figs. 1 and 2; Table 1). The PS_{b-a} values of [^{3}H]taurocholate (1 μM), and CDCGamF and CGamF (10 μM), in LLC-NTCP/BSEP were significantly greater than those in control LLC-PK1 cells and NTCP-expressing LLC-PK1 (LLC-NTCP) cells, indicating that these bile acids are good substrates of BSEP. In contrast, for CamF, UDC-L-NBD (10 μM), and 7β-NBD-NCT (10 μM), transport by NTCP and BSEP was barely detectable.

The value of PS_{b-a} in LLC-NTCP/BSEP was the highest when [^{3}H]taurocholate was used. The absolute PS_{b-a} value of all the fluorescent bile acids was less than ⅙ that of [^{3}H] taurocholate. The ratio of the PS_{b-a} value of LLC-NTCP/BSEP to that of LLC-NTCP was 4.8-fold for [^{3}H]taurocholate, 2.6-fold for CGamF, and 1.8-fold for CDCGamF (Fig. 2, bottom graph). These results indicate that taurocholate is a better substrate for the subsequent inhibition studies. Furthermore, labeled compounds are better tools for measuring the intracellular content of the compounds, which is important for this study because it is needed to calculate the efflux clearance across the apical membrane (PS3).

Inhibitory Effects of a Series of Cholestasis-Inducing Drugs. Next, the inhibitory effect of cholestasis-inducing drugs on the basal-to-apical transport clearance PS_{b-a} of taurocholate was examined (Fig. 3). PS_{b-a} was reduced by 100 μM rifampicin and rifamycin SV to 50% of the control level, and 10 μM glibenclamide reduced it to 70% (Fig. 3A). The intracellular concentration (C_{cell}) of taurocholate was determined for each compound at the end of the experiment (Fig. 3B). The C_{cell} of taurocholate was increased by 100 μM rifampicin to 160% of that of control cells (no inhibitor added). However, 100 μM rifamycin caused a 10% reduction in the apparent cellular concentration of taurocholate and 10 μM glibenclamide led to a 30% reduction in C_{cell} compared with control cells. Calculation of the efflux clearance across the apical membrane PS3 using the measured C_{cell} showed that 100 μM rifampicin, rifamycin SV, and glibenclamide produced a 70%, 44%, and 63% inhibition of PS3, respectively, indicating that the drugs inhibited the efflux of taurocholate by BSEP located in the apical membrane (Fig. 3C). When the efflux process is the only target of inhibition, C_{cell} should be increased by the drugs compared with untreated LLC-NTCP/BSEP cells. However, as mentioned above, C_{cell} was reduced by rifamycin SV and glibenclamide. This means that not only BSEP but also NTCP was inhibited in this experiment as far as rifamycin SV and glibenclamide were concerned. Of course, from these data, we cannot exclude the possibility that inhibition of NTCP is also involved in the case of rifampicin. A 100 μM concentration of captopril and cimetidine did not affect the transport and C_{cell} of taurocholate significantly (Fig. 3, A–C).

Kinetics of the Inhibition by Cyclosporin A. To evaluate the inhibition kinetics involved in the transcellular transport when both the uptake and efflux processes are affected, cyclosporin A, an inhibitor of both NTCP and BSEP, was also examined (Fig. 4). The basal-to-apical transport clearance PS_{b-a} of taurocholate was inhibited by cyclosporin A (and its metabolites) with a K_i value of 1.0 ± 0.2 (μM) (Fig. 4A). The intracellular concentration C_{cell} determined at the end of each experiment was also reduced by cyclosporin A, suggesting that uptake of taurocholate by NTCP was inhibited by cyclosporin A treatment. The inhibition of the uptake process was confirmed by evaluating the inhibitory effect of cyclosporin A on the uptake of taurocholate into only NTCP-expressing LLC-PK1 cells. The K_i value was determined as 0.27 ± 0.06 (μM) (Fig. 4C). At the same time, the calculated PS3 showed a reduction depending on the concentration of cyclosporin A, probably because of inhibition of BSEP by cyclosporin A (and/or its metabolites) (Fig. 4B). These results showed that both uptake and efflux processes are affected by 1 to 10 μM cyclosporin A.

Discussion

In the present study, we assessed the inhibitory effects of cholestasis-inducing drugs on bile acid transport across LLC-NTCP/BSEP cells. Our hope was to develop a rapid screening system for drugs that inhibit these transporters.

Initially, we focused on the fluorescent bile acids as a probe of NTCP and BSEP function and investigated whether they were substrates of NTCP and BSEP using LLC-NTCP/BSEP. The fluorescent derivatives of bile acids used in this study were originally synthesized for the functional analysis of bile salt transport systems in isolated hepatocytes, immortalized cell lines derived from hepatocytes, or in vivo (Holzinger et al., 1998; Cantz et al., 2000). Direct demonstration of the transport of these bile acids via NTCP or BSEP has not yet been carried out, although sodium-dependent uptake for CGamF has been observed (Maglova et al., 1995).

Basal-to-apical transport across LLC-NTCP/BSEP was observed in a rank order of taurocholate > CGamF > CDCGamF, and no significant transport was observed for UDC-L-NBD, CamF, and 7β-NBD-NCT (Fig. 2). This order was similar to that of the maximum output rate of the bile acids in an isolated liver perfusion study: taurocholate 22.7 > CGamF 14.1 > CamF 7.7 > UDC-L-NBD 1.1 (nmol/g liver/min) (Holzinger et al., 1998). This result supports the hypothesis that the transport of fluorescent derivatives of cholic acid in hepatocytes is mainly mediated by NTCP and BSEP, and showed that our in vitro system can reflect the physiological function of these transporters as far as transcellular transport is concerned. As for UDC-L-NBD, although uptake by LLC-NTCP inhibited by taurocholate was observed using fluorescent microscopy (data not shown), no significant transcellular transport across LLC-NTCP/BSEP was observed. This might be because of the nature of this bile salt, which is sequestered in the cells (Holzinger et al., 1998; Cantz et al., 2000). Nonetheless, fluorescent bile acids were transported in this system. Better fluorescent bile acids that will be transported as efficiently as taurocholate will make excellent tools for high-throughput screening.

Inhibition of BSEP by cholestasis-inducible drugs is one of the most frequently reported mechanisms of drug-induced cholestasis (Bohan and Boyer, 2002). Among such drugs, rifampicin, rifamycin SV, glibenclamide, and cyclosporin A (Stieger et al., 2000; Byrne et al., 2002) were used in this study. As shown in Fig. 3, PS3, the efflux clearance that reflects the function of BSEP, was reduced by all the drugs examined. The concentration needed for 50% inhibition of PS3 is between 10 and 100 μM for rifampicin and glibenclamide and approximately 100 μM for rifamycin SV. The reported K_i values for the inhibition of taurocholate uptake into human BSEP-expressing membrane vesicles are 31 μM for rifamycin SV and 31 μM for glibenclamide (Byrne et al., 2002). For rifampicin, only the K_i value of 12 μM for rat Bsep is available (Stieger et al., 2000). Compared

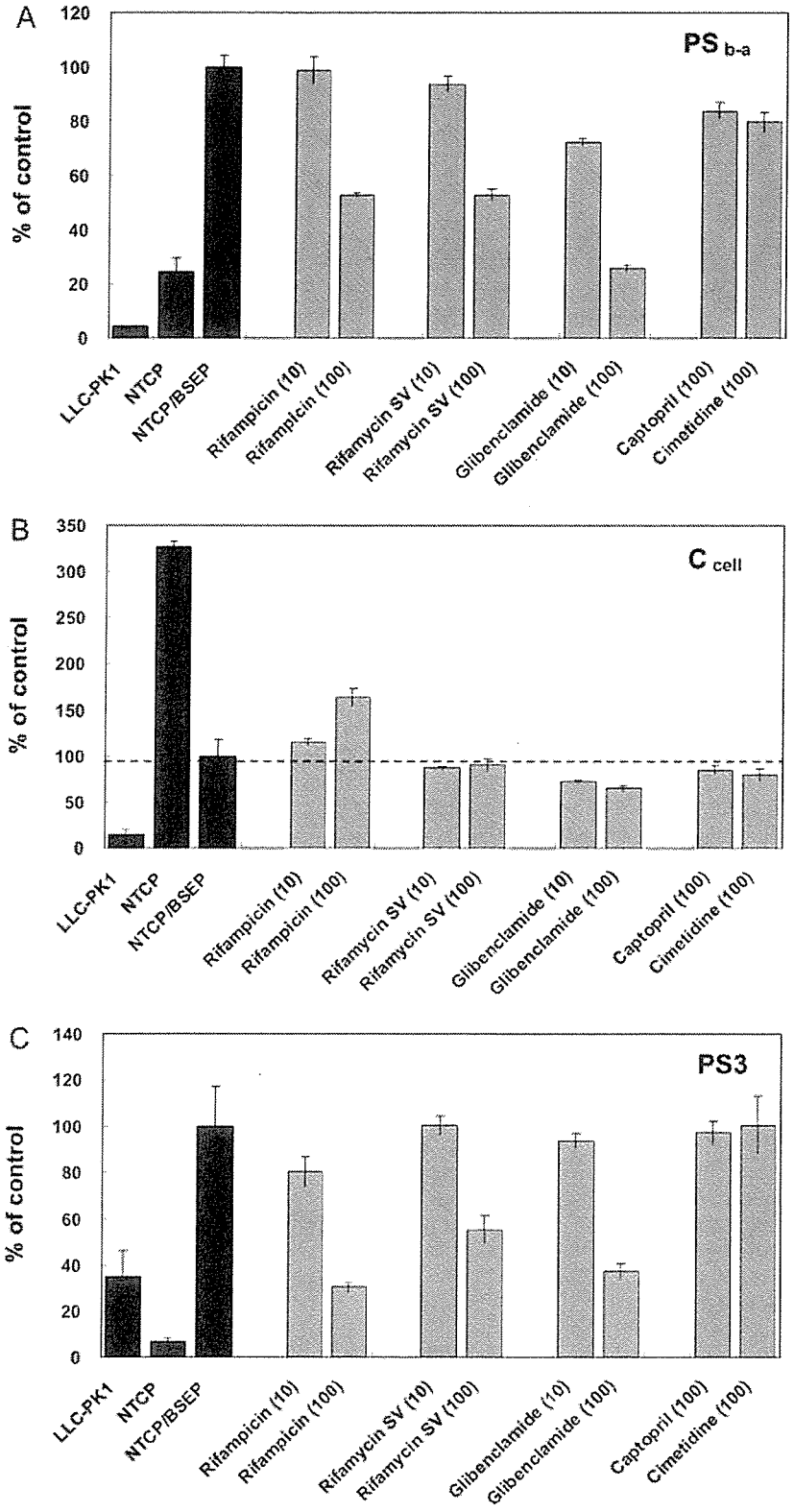

FIG. 3. Inhibitory effects of cholestasis-inducing drugs on the transport of taurocholate across NTCP- and BSEP-coexpressing LLC-PK1 cells. Basal-to-apical transport clearance $PS_{b\text{-}a}$ (A), intracellular concentration C_{cell} (B), and apical efflux clearance PS3 (C) of taurocholate in LLC-PK1, LLC-NTCP, and LLC-NTCP/BSEP cell monolayers were determined at 60 min (closed bars). Inhibitory effects of 10 or 100 μM concentrations of various drugs on LLC-NTCP/BSEP were studied (open and hatched bars). The drugs were added to the apical and basal compartment 30 min before applying taurocholate.

with these values, the inhibitory concentration was higher in our LLC-NTCP/BSEP cells than in other studies that used vesicles. One possible explanation for this is that the protein unbound concentrations of the drugs in cytoplasm are lower than in the medium because the drugs may not penetrate the plasma membrane efficiently and the drugs may also bind to intracellular proteins.

Inhibition of BSEP in the transcellular transport of taurocholate should be accompanied by an increase in the intracellular concentration of taurocholate. However, the increase was observed only in the case of rifampicin. This means that rifamycin SV and glibenclamide also inhibited NTCP-mediated uptake at the same time. Recently, it has been reported that 100 μM rifampicin or rifamycin SV can reduce